TECHNICAL SUMMARY REPORT

TO

ADVANCED RESEARCH PROJECTS AGENCY

ON

MATERIALS PREPARATION AND CHARACTERIZATION RESEARCH

For the period 1 July 1966 to 30 June 1967

Contract No. DA-49-083 OSA-3140

ARPA Order No. 338, Amendment 2

THE MATERIALS RESEARCH LABORATORY

THE PENNSYLVANIA STATE UNIVERSITY

UNIVERSITY PARK, PENNSYLVANIA

Technical Summary Report

To

ADVANCED RESEARCH PROJECTS AGENCY

On

Materials Preparation and Characterization Research

For the period 1 July 1966 to 30 June 1967

Contract No. DA-49-083 OSA-3140

ARPA Order No. 338, Amendment 2

Contract issued by:
Department of the Army
Defense Supply Service - Washington
Room 1D243, The Pentagon
Washington 25, D. C.

Contract Amount: $500,000
Contract Dated: 10 February 1966
Expiration Date: 30 June 1967

Rustum Roy
The Pennsylvania State University
Materials Research Laboratory
1-112 Research Unit No. 1
University Park, Pennsylvania 16802

Telephone: 814-865-3422

Table of Contents

1.0 INTRODUCTION

1.1 Nature of this Report

This report covers in detail the work supported by Contract DA-49-083 OSA-3140, for the last year July 1, 1966 - June 30, 1967, and also represents the Final Report for the two-year period ending on the same date.

In addition, this report, following a practice initiated earlier, includes a very brief summary of the overall research activity within the Materials Research Laboratory, as indicated by graduate students trained and research published. The relationship between the ARPA-supported work on "Preparation and Characterization" as the cement which ties together much of the work in the laboratory will be evident from the comparison of these two aspects of the report.

1.2 Summary of Overall Research Effort in the Materials Research Laboratory

We list below some of the main developments during the year, the faculty active in the MRL, and the data on graduate student training. There are also appended a list of papers appearing in print during the last year.

Two new faculty members have been added to the laboratory. Dr. R. E. Newnham, formerly Associate Professor of Electrical Engineering at Massachusetts Institute of Technology joined the laboratory in September 1966 as Associate Professor of Solid State Science. Professor Newnham is a crystal physicist and crystallographer who has been studying the relationship of optical and magnetic properties to structure. He is involved in various aspects of X-ray and optical characterization work under this contract. Dr. J. W. Faust Jr., formerly of the Westinghouse Research Laboratories, joined the faculty on February 1 as Professor of Solid State Science.

Professor Faust has been associated with the successful twin-plane re-entrant edge growth of silicon ribbon from its earliest days. He has also been in charge of the "Characterization Laboratory" at Westinghouse and is well known for his work on etching of semiconductors.

Ground was broken for the new building which will accommodate the Materials Research Laboratory in the Fall of 1968. Major new items of equipment which were acquired during the year included a Scanning Electron Microscope (JEOL), automated outputs for X-ray equipment, Photometer for Laser Ultramicroscope, low temperature He cryostats, and Lang Camera.

1.2.1 Highlights: Research

The laboratory continues to be one of the major focal points for an effective interdisciplinary approach to the science of non-metallic solids. Items of especial interest among the 'preparation' aspects of the work during this year include the tailormaking for the first time of transparent photoconducting oxide glasses without any variable valence ions - a substantial advance for the use of glasses as electronically-active solids; the synthesis of Ni_3TeO_6, a possible ferroelectric compound, and the preparation of a wide range of novel glasses including those containing several mole % of inert gases. Among characterization projects, it is worth noting that in Maiman's recent review (Physics Today, June 1966), of the five promising applications of the laser singled out for mention, one was the laser T-O-F mass spectrometer developed here. Another outstanding strength in this area are the new computer-search programs for identifying complex materials from powder X-ray data, under continuous development in our laboratories with ASTM support. Under the heading of properties of materials, the following titles indicate some of the areas of substantial

advance: field-enhancement of radiation dosimetry; new theory of "ferroelectric" relaxor materials; precision optical and elastic measurements under pressure.

1.2.2 Communications

We continue our work in post-doctoral continuing education in materials preparation and characterization through our two-week summer course, and our formalized interaction with industry through our Industrial Coupling Program - both of these efforts have been described previously.

Several faculty members in the laboratory are convinced that the neglect of the chemistry (structure and composition) of materials is a major handicap in the optimum development of Materials Science in this country. To this end several actions have been undertaken:

a. The new Journal, "Materials Research Bulletin", edited by Professors H. K. Henisch and Rustum Roy, and published by Pergamon Press, was launched in September 1966. The journal innovates by using a non-refereeing system by sending in papers to be communicated by any one of 25 Associate Editors and also by using photo-offset direct from the manuscript for all papers. Achievement of an approximate lead time of only six weeks from receipt of paper to publication, and monthly publication from the first issue, with a total of probably 900 pages of text in the first year, attest to the pre-existing need for a Journal in this field of "Crystal Growth, and Materials Preparation and Characterization".

b. Prof. Rustum Roy served as one of six members of the NAS-NRC Materials Advisory Board Committee on Characterization of Materials, and was the Chairman of the Panel on Structural Characterization.

Prof. W. R. Buessem served on the Panel on Characterization of Polycrystalline Materials. The reports of the panels and the committee have been described as constituting a "landmark in the analysis of the needs of materials science and engineering".

c. In November 1966, the first International Conference on the Characterization of Materials" was held at Penn State under ARPA sponsorship. The group of scientists was distinguished by its marked interdisciplinary nature and the meeting proved to be effective. Since then, plans have been made for the next meeting in November 1967 in Rochester, New York.

d. Due to the increasing research activity in the Materials Research Laboratory with non-crystalline solids, the possibility of a cooperative program between ourselves and a government laboratory and industry was mooted last year. This has developed now into a reality which goes into effect July 1, 1967.

1.2.3 Graduate Student Support

Approximately 80 graduate students have been supported financially (a few for part of the year only) during the last fiscal year. Most of these have been working for Ph.D. degrees in the following fields: Solid State Technology, (= Materials Science), Physics, Engineering Mechanics, Electrical Engineering, Geochemistry, and Chemistry. In addition we have employed nearly a dozen undergraduate students in serious research participation during the summer months.

1.2.4 Graduate Degrees Awarded

During this year (July 1, 1966 - June 30, 1967) 10 graduate students within the M.R.L. received Ph.D. degrees and 6 earned M.S. degrees. These

are listed below. Most, but not all the students are taking their degrees within a wholly new curriculum. The rate of build-up of this Solid State degree program has been truly remarkable. The program was authorized by the Graduate School in 1960 with the first Ph.D. degrees being granted in 1963. Only three years later, this program became the third largest producer of Ph.D.'s in the University - behind Chemistry (1) and Physics (2). The growth of this degree program has been intimately related to the research activity of the Materials Research Laboratory, and hence in a major way to the ARPA contract. It should be noted that this growth specifically in the number of trained materials scientists is superimposed upon the general growth (which has also been aided in some cases by the Materials Research Laboratory) of several other departments in this University, which train personnel in fields related to materials science. i.e. physics, engineering mechanics, metallurgy, and ceramics, none of which was subsumed under the Solid State program.

1.2.5 Faculty involved

G. R. Barsch - Associate Professor of Solid State Science

G. W. Brindley - Professor of Solid State Technology

W. R. Buessem - Professor of Ceramic Science

L. E. Cross - Associate Professor of Solid State Science

F. Dachille - Associate Professor of Geochemistry

J. W. Faust Jr. - Professor of Solid State Science

H. K. Henisch - Professor of Applied Physics

M. C. Inman - Associate Professor of Engineering Mechanics

G. G. Johnson - Assistant Professor of Solid State Technology

B. E. Knox - Assistant Professor of Solid State Technology

H. A. McKinstry - Assistant Professor of Solid State Technology

A. Muan - Professor of Metallurgy

L. N. Mulay - Associate Professor of Solid State Science

R. E. Newnham - Associate Professor of Solid State Science

D. M. Roy - Senior Research Associate in Geochemistry

R. Roy - Professor of Geochemistry and Director, Materials Research Laboratory

V. Vand - Professor of Crystallography

F. Vastola - Associate Professor of Fuel Science

K. Vedam - Associate Professor of Solid State Science

P. Walker Jr. - Professor of Fuel Science

J. N. Weber - Assistant Professor of Geochemistry

E. W. White - Assistant Professor of Solid State Science

W. B. White - Assistant Professor of Geochemistry

1.2.6 Degrees Granted

Ph.D.

Name	Thesis Title
Balgord, William Dwyer	"Crystal Chemical Relationships in the Analcite Family and a Study of Cation-H_2O Coordination in Certain Synthetic and Natural Zeolites."
Grosewald, Peter Samuel	"Transport Properties of Graphite as Affected by Temperature and Boronation."
Harvill, Marvin Lavell	"Hydrothermal Crystal Growth of Rutile Structure Oxides TiO_2, GeO_2 and SiO_2."
Lussow, Robert Otis	"The Reaction of Oxygen with Graphon."
Noble, Wendall Phillips	"The Structure and Properties of Cleaved Semiconductor Surfaces."

Rose, Millard Franklin	"The Effect of Strong Shock Waves on Polycrystalline Nickel."
Taylor, Raymond Ellory	"The Dynamic Mechanical Behavior of Graphites and Carbons."
Wentworth, Sally Ann	"An Investigation of Fine-Grained Micas with Emphasis on Their Hydrous Character."

M.S.

Groner, Carl Fred	"A Non-Contact Method for Dielectric Measurements."
Srinivasagoplan, Chellappa	"Photoconduction in Gel-Grown Lead Iodide."

1.2.7 Research Papers Published by the Faculty

Achar, B. N. N., G. W. Brindley, J. H. Sharp. "Kinetics and Mechanism of Dehydroxylation Processes. III. Applications and Limitations of Dynamic Methods." Proc. Internat. Clay Conf. (Jerusalem, Israel) 1:67-73 (1966).

Barry, T. L., R. Roy. "Observations on Densification of Ionic Solids by Cold-Pressing at Ultrahigh Pressures." J. Canad. Ceram. Soc. 35:32-35 (1966).

"Defect Characterization in and Precipitation from $CaO:Yb_2O_3$ Crystalline Solutions." J. Am. Ceram. Soc. 50:105-108 (1967).

Barry, T. L., V. S. Stubican, R. Roy. "Phase Equilibria in the System $CaO - Yb_2O_3$." J. Am. Ceram. Soc. 49:667-670 (1966).

Barsch, G. R. "Adiabatic, Isothermal and Intermediate Pressure Derivatives of the Elastic Constants for Cubic Symmetry. I. Basic Formulae." Phys. Stat. Solidi 19:129-139 (1967).

Barsch, G. R., Z. P. Chang. "Adiabatic, Isothermal, and Intermediate Pressure Derivatives of the Elastic Constants for Cubic Symmetry. II. Numerical Results for 25 Materials." Phys. Stat. Solidi 19:139-151 (1967).

Berkes, J. S., W. B. White. "The Optical Spectrum of Nickel in Alkali Tetraborate Glasses." Phys. Chem. Glasses 7:191-199 (1966).

Bigelow, W. C. (U. of Michigan), G. G. Johnson Jr. "Trial Revision of Fink Index," Special Publication for the Joint Committee on Chemical Analysis by Powder Diffraction Methods, ASTM (Limited Publication) 714 pp. (1966).

Biggers, J. V., A. Muan. "Activity-Composition Relations in Orthosilicate and Metasilicate Solid Solutions in the System MnO-CoO-SiO_2." J. Am. Ceram. Soc. 50:230-235 (1967).

Bratton, R. J., G. W. Brindley. "Kinetics of Vapour Phase Hydration of Magnesium Oxide. Part 3. Effect of Iron Oxides in Solid Solution." Trans. Faraday Soc. 62:2909-2915 (1966).

Braun, I., H. K. Henisch. "Characteristics of Injecting Point Contacts on Semiconductors. I. In Darkness." J. Solid State Elec. 9:981-987 (1966).

"Characteristics of Injecting Point Contacts on Semiconductors. II. Under Illumination." J. Solid State Elec. 9:1111-1117 (1966).

Brindley, G. W. "Discussions and Recommendations Concerning the Nomenclature of Clay Minerals and Related Phyllosilicates." Clays and Clay Min. Proc. 14th Nat. Conf. (Berkeley, Calif.), pp. 27-34 (1966).

"Kinetics and Mechanisms of Some Mineral Dehydroxylation Reactions." Internat. Symp. on Reaction Mechanisms of Inorganic Solids (Aberdeen, Scotland) 2:1-6 (1966).

"On Fears and Freedoms." Univ. of Leeds Rev. 10:112-113 (1966).

"Purpose of the Master's Degree." Phys. Today 20:11-12 (1967).

Brindley, G. W., P. de Souza Santos (U. of Sao Paulo). "New Varieties of Kaolin-Group Minerals and the Problem of Finding a Suitable Nomenclature." Proc. Internat. Clay Conf. (Jerusalem, Israel) 1:3-9 (1966).

Brindley, G. W., J. H. Sharp, J. H. Patterson, B. N. N. Achar. "Kinetics and Mechanism of Dehydroxylation Processes. I. Temperature and Vapor Pressure Dependence of Dehydroxylation of Kaolinite." Am. Mineral. 52:201-211 (1967).

Buessem, W. R. "Electroceramics Today." Mineral Industries 36:1-6 (1967).

Buessem, W. R., F. F. Lange. "Residual Stresses in Anisotropic Ceramics." Interceram. 15:229-231 (1966).

Chung, D. H., W. R. Buessem. 'The Elastic Anisotropy of Crystals." J. Appl. Phys. 38:2010-2012 (1967).

Cross, L. E. "Ferroelectric Relaxation Dielectrics." J. Canad. Ceram. Soc. 34:142-147 (1965).

"Dielectric Measurement Techniques." Materials Research Laboratory Publication, PSU, 42 pp. (1966).

"Antiferroelectric-Ferroelectric Switching in a Simple 'Kittel' Antiferroelectric." J. Phys. Soc. Japan 22:(6) (1967).

Darrow, M. S., W. B. White, R. Roy. "Phas Relations in the System PbS-PbTe." AIME 236:654-658 (1966).

Dennis, J., H. K. Henisch. "Nucleation and Growth of Crystals in Gels." J. Electrochem. Soc. 114:263-266 (1967).

Farrell, E. F., R. E. Newnham. "Electronic and Vibrational Absorption Spectra in Cordierite." Amer. Min. 52:380-388 (1967).

Faile, S. P., D. M. Roy. "Solubilities of Ar, N_2, CO_2, He in Glasses at Pressures to 10 Kbars." J. Am. Ceram. Soc. 49:638-644 (1966).

Faust, J. W., Jr., H. F. John, R. Stickler. "The Role of Microdefects in Silicon Starting Materials as Quality Reducing Factors in Semiconductor Devices" in "Physics of Failure in Electronics." (M. E. Goldberg and J. Vaccaro, eds.), pp. 367-378 vol.4, published by U.S.A.F. (1966).

Faust, J. W., Jr. "Crystal Growth Utilizing the Twin Plane Re-entrant Edge Mechanism" in "Crystal Growth" (H. Peiser, ed.). pp. 183-185, Pergamon Press, Oxford (1967).

Faust, J. W., Jr. "The Etching of $Bi_{2-y}Sb_yTe_xSe_{(3-x)}$." Praktishe Metallographie 3:381-386 (1966).

Faust, J. W., Jr., R. Stickler. "Techniques for Measuring the Twin Spacing in Dendrite, and Webs of Semiconductors." Praktishe Metallographie 4:137-143 (1967).

Greer, R. T., B. W. Hapke (Cornell U.). "Electron Microprobe Analyses of Powder Darkened by Simulated Solar-Wind Irradiation." J. Geophys. Res. 72:32-33 (1967).

Hanawalt, J. D. (U. of Michigan), G. G. Johnson Jr. "Overlapping HANEX." Spec. Publication for the Joint Committee on Chemical Analysis by Powder Diffraction Methods. ASTM (Ltd. Pub.) 230 pp. (1966).

Hanoka, J., K. Vedam, H. K. Henisch. "Polytypism in Gel-Grown Lead Iodide Crystals." Proc. Int. Conf. on Crystal Growth (Boston, Mass.), June 1966. J. Phys. Chem. Solids Suppl. pp. 369-371 (1967).

Harvill, M. L., R. Roy. "Habit of Hydrothermally Grown Rutile Structure Crystals in the Light of the Hartman Theory and its Extension," in Chapter G2 of Crystal Growth. Proc. Int. Conf. on Crystal Growth (Boston, Mass.), Ed. H. Steffen Peiser, NBS and Harvard University, pp. 563-567 (1966).

Henisch, H. K., S. Srinivasagopalan. "Properties of Semiconducting Lead Iodide." Solid State Comm. 4:415-418 (1966).

Inman, M. C. "Application of Transmission Electron Microscopy to Studies of Relative Interfacial Energies in Solids." Mat. Sci. Res. 3:175-186 (1960).

Inman, M. C., L. E. Murr. "Effects of Vacuum Environment on the Sub-Structure of Evaporated F.C.C. Metal Films." Phil. Mag. 14:135-153 (1966).

Inman, M. C., L. E. Murr, M. F. Rose. "Investigation of Sub-Structure of Stainless Steel after Explosive Shock Deformation." ASTM STP 396:39 (1966).

John, H. F., J. W. Faust Jr., R. Stickler. "Microinhomogeneity Problems in Silicon," IEEE Trans. on Parts, Materials, and Packaging, PMP 2:51-58 (1966).

Johnson, G. G., Jr., J. D. Hanawalt (U. of Michigan). "Decreasing HANEX." Special Publication for the Joint Committee on Chemical Analysis by Powder Diffraction Methods. ASTM (Ltd. Pub.), 177 pp. (1967).

Johnson, G. G., Jr., V. Vand. "A FORTRAN Powder Diffraction Identification System." Pittsburgh Diffraction Conference Paper B-1 (1966).

"A KWIC Guide to the Inorganic Powder Diffraction File." ASTM Special Publication No. PDIS-16K, 374 pp. (1967).

"A FORTRAN II System for the Identification of Unknown Multiphase Powder Diffraction Patterns." Materials Research Laboratory Publication, PSU, 66 pp. (1967).

"Application of a Fourier Data Smoothing Technique to the Meteoritic Crater Ries Kessel." J. Geophys. Res. 72:1741-1750 (1967).

"FORTRAN II Programs for the Identification of Multiphase Unknown Powder Diffraction Patterns Using the Joint Committee's Powder Diffraction File." ASTM, 30 pp. (1967).

Jones, T. S. (Allegheny Ludlum Steel Corp., Brackenridge, Pa.), S. Kimura, A. Muan. "Phase Relations in the System FeO-Fe_2O_3-VrO_2-SiO_2." J. Am. Ceram. Soc. 50:137-142 (1967).

Katz, G., R. Roy. "Flux Growth and Characterization of β-Ga_2O_3 Single Crystals." J. Am. Ceram. Soc. 49:168-169 (1966).

Knox, B. E. "Bond Energies and Bond Dissociation Energies." The Encyclopedia of Chemistry, 2nd. Ed., Reinhold Pub., N. Y., p. 139 (1966).

Lange, F. F., W. R. Buessem. "Intrinsic Brittle Strength of MgO Bicrystals." J. Appl. Phys. 38:2013-2019 (1967).

Masse, D. T. (Escola De Minas, Brazil), E. Rosen (U. of Umeå, Sweden), A. Muan. "Activity-Composition Relations in Co_2SiO_4-Fe_2SiO_4 Solid Solutions at 1180°C." J. Am. Ceram. Soc. 49:328-329 (1966).

McCarthy, G. J., W. B. White, R. Roy. "Preparation of $Sm_4(SiO_4)_3$." J. Inorg. Nucl. Chem. 29:253-254 (1967).

Miller, R. O., F. Dachille, R. Roy. "High-Pressure Phase-Equilibrium Studies of CdS and MnS by Static and Dynamic Methods." J. Appl. Phys. 37:4913-4918 (1966).

Miyashita, K., H. K. Henisch, J. Toole. "Use of Diamond for Photo-Stimulated UV Radiation Dosimetry." J. Solid State Elec. 10:193-197 (1967).

Morris, A. E. (U. of Missouri), A. Muan. "Phase Equilibria in the System MnO-Mn_2O_3-SiO_2." J. Metal. 18:957-960 (1966).

Muan, A. 'Activity-Composition Relations in Some Oxide and Alloy Phases at Elevated Temperatures." Thermodynamics, Inter. Atomic Agency (Vienna) 2:547-560 (1966).

Mulay, I., L. N. Mulay, J. C. Hunter (Natl. Institute of Health). "Magnetic Susceptibility and E.S.R. Absorption Spectra of S-91 and S-91A Mouse Melanoma Tumors." Phys. Med. Biol. 11:(4):620-621 (1966).

Mulay, L. N. "Magnetic Phenomena" in Encyclopedia of Chemistry, Second Edition, Ed. George Clark, Reinhold Pub. Co., pp. 627-630 (1966).

"Magnetic Susceptibility" in Encyclopedia of Industrial Chemical Analysis 2:445-464, Ed. F. D. Snell and C. L. Hilton, John Wiley & Sons, Inc. (1966).

Mulay, L. N., N. L. Hofmann. "Magnetic Susceptibility, E.P.R. and Crystal Structure Studies on Binuclear Complexes of Fe(III)." Inorg. Nucl. Chem. Letters 2:189-192 (1966).

Mulay, L. N., L. K. Keys. "Magnetic Studies of the Semiconductor of Metal Transitions in Ti_3O_5." Appl. Phys. Let. 9:248-250 (1966).

"Magnetic Susceptibility Measurements on Rutile and the Magneli Phases of TiO_2." Phys. Rev. 154:453-456 (1967).

"Magnetic Susceptibility Studies on the Magneli Phases of the Titanium-Oxygen System." J. Appl. Phys. 38:(3):1466 (1967).

"Magnetism of the Titanium-Oxygen System." Jap. J. Appl. Phys. 6:122 (1967).

"Magnetism and the Metal-Semiconductor Transition in Ti_3O_5." Bull. Am. Phys. Soc. XII:(4):503 (1967).

Myers, M. B., K. Vedam. "Effect of Pressure on the Optical Rotatory Power and Dispersion of α-Quartz." J. Opt. Soc. Am. 56:1741-1742 (1966).

Nandi, S. P., P. L. Walker Jr. "Diffusion of Argon from Coals of Different Rank." Coal Science, Advances in Chemistry Series No. 55:379-385 (1966).

Nelson, E. T., Jean Worrall, P. L. Walker Jr. "Coal Science," Advances in Chemistry Series No. 55:602-620 (1966).

Newnham, R. E. "Crystal Structure of $ZiTiO_4$." J. Am. Ceram. Soc. 50:216 (1967).

Newnham, R. E., L. G. Caron, R. P. Santoro. "Magnetic Properties of $CaCoSiO_4$ and $CaFeSiO_4$," J. Amer. Ceram. Soc., 49:284-285 (1966).

Newnham, R. E., R. P. Santora, P. F. Seal, G. R. Stallings. "Antiferromagnetism in $Mn_3B_2O_6$, $Co_3B_2O_6$ and $Ni_3B_2O_6$." Phys. Stat. Sol. 16:K17-K19 (1966).

Newnham, R. E., R. P. Santoro. "Magnetic and Optical Properties of Dioptase," Phys. Stat. Solidi. 19:K87-K90 (1967).

Newnham, R. E., E. P. Meagher. "Crystal Structure of Ni_3TeO_6." Mat. Res. Bull. 2:549-554 (1967).

Noble, W. P., Jr., I. Braun, H. K. Henisch. "Contract Barriers on Cleaved Germanium Surfaces." J. Solid State Elec. 10:45-48 (1967).

Perry, F. W. (Sprague Electric, North Adams, Mass.), G. A. Hutchins (Sprague Electric), L. E. Cross. "Compositional Inhomogeneity of (Ba,Pb)TiO_3 Crystals." Mat. Res. Bull. 2:409-418 (1967).

Prosser, V., H. K. Henisch. "Long Wavelength Side of the Absorption Edge in Hexagonal Selenium." Mat. Res. Bull. 1:283-292 (1966).

"Diffuse Reflectivity of Selenium." Mat. Res. Bull. 2:75-84 (1967).

Ragone, S. E., R. K. Latta, D. M. Roy, O. F. Tuttle. "The System K_2CO_3-$MgCO_3$." J. Phys. Chem. 30:3351-3361 (1966).

Robinson, L. B., W. B. White, R. Roy. "Growth of Transition Metal Oxide Crystals by Halide Vapour Hydrolysis." J. Mat. Sci. 1:336-345 (1966).

Rouxhet, P. G., G. W. Brindley. "Experimental Studies of Fine-Grained Micas. I. Organic Contamination on the Surface of Wet-Ground Muscovite." Clay Min. 6:211-218 (1966).

"Experimental Studies of Fine-Grained Micas. II. The Water Content of Wet-Ground Micas." Clay Min. 6:219-228 (1966).

Roy, D. M., R. E. Barks. "Single Crystal Growth of R_2O_3 (Corundum Structure) Oxides by the Flux Method," in "Crystal Growth." Proc. Int. Conf. on Crystal Growth (Boston, 1966). Suppl to J. Phys. Chem. Solids, Pergamon Press (1967).

Roy, R. "Application of the Isothermal Flux Evaporation Method." Mat. Res. Bull. 1:299-302 (1966).

Roy, R., R. T. Greer. "Proton Trapping in TiO_2 and Simple Oxides." Sol. State Comm. 5:109-111 (1967).

Sagar, A., J. W. Faust Jr. "Dislocation Studies in Bi_2Te_3 by Etch Pit Techniques," J. Appl. Phys. 38:482-490 (1967).

Sagar, A., R. Ure, J. W. Faust Jr. "An Etch for Dislocations in Bi_2Te_3," Praktishe Metallographie, 4:35-39 (1967).

Sagar, A., J. W. Faust Jr. "Direct Observation of Dislocation Loops from Frank-Read Source in Bi_2Te_3," Phys. Letters 23:406-408 (1966).

Sagar, A., J. W. Faust Jr. "A Study of the Discrepancy from a Perfect Match in the Etch Patterns on the Opposite Cleavage Faces in Bi_2Te_3," J. Appl. Phys. 38:2240-2243 (1967).

Sagar, A., J. W. Faust Jr. "Observation of Dislocations Piled up against a Low Angle Boundary in Bi_2Te_3," J. Appl. Phys., May.

Sagar, A., J. W. Faust Jr. "Investigation of Cu Diffusion in Bi_2Te_3 by Etching Techniques," J. Appl. Phys., May.

Santoro, R. P., R. E. Newnham, S. Nomura. 'Magnetic Properties of Mn_2SiO_4 and Fe_2SiO_4." J. Phys. Chem. Solids 27:655-666 (1966).

Santoro, R. P., D. J. Segal, R. E. Newnham. "Magnetic Properties of $LiCoPO_4$ and $LiNiPO_4$." J. Phys. Chem. Solids. 27:1192-1193 (1966).

Santoro, R. P., R. E. Newnham. "Antiferromagnetism in $LiFePO_4$." Acta Cryst. 22:344-347 (1967).

Santoro, R. P., R. E. Newnham. "Survey of Magnetoelectric Materials." Technical Report AFML-TR-66-327. September 1966. 24 pp.

Schlaudt, C. M., D. M. Roy. "The Join Ca_2SiO_4-$CaMgSiO_4$." J. Am. Ceram. Soc. 49:430-432 (1966).

Schmidt, E. D. D., K. Vedam. "Variation of the Refractive Indices of CaF_2, BaF_2 and β-PbF_2 with Pressure to 7 Kbars." J. Phys. Chem. Sol. 27:1563-1566 (1966).

Segal, D. J., R. P. Santoro, R. E. Newnham. "Neutron-Diffraction Study of $Bi_4Si_3O_{12}$." Zeit. für. Krist. 123:73-76 (1966).

Sharp, J. H., G. W. Brindley, B. N. N. Achar. "Numerical Data for Some Commonly Used Solid State Reaction Equations." J. Am. Ceram. Soc. 49:379-382 (1966).

Shelef, M., P. L. Walker Jr. "Transient Phenomena in the Gasification of Graphite by High Purity Carbon Dioxide." Carbon 5:93-105 (1967).

Slagle, O. D., H. A. McKinstry. "The Lattice Parameter in Solid Solution KCl-KBr." Acta Cryst. 21:1013-1020 (1966).

"The Temperature Dependence of the Elastic Constants of the Alkali Halides. I. NaCl, KCl and KBr." J. Appl. Phys. 38:437-446 (1967).

"The Temperature Dependence of the Elastic Constants of the Alkali Halides. II. The Solid Solution of KCl-KBr." J. Appl. Phys. 38:446-451 (1967).

"The Temperature Dependence of the Elastic Constants of the Alkali Halides. III. CsCl, CsBr and CsI." J. Appl. Phys. 38:451-458 (1967).

Souza Santos, P. de, Helena de Souza Santos (U. of Sao Paulo, Brazil), G. W. Brindley. "Mineralogical Studies of Kaolinite-Halloystie Clays. Part IV. A Platy Mineral with Structural Swelling and Shrinking Characteristics." Am. Mineral. 51:1640-1648 (1966).

Stacy, W. O., G. R. Imperial, P. L. Walker Jr. "Chlorine Fixation on Anthracites and Carbon Blacks and Its Effect on Electrical Resistivity." Carbon 4:343-352 (1966).

Stickler, R., J. W. Faust Jr. "Comparison of Two Different Techniques to Determine the Depth of Damage," Electrochem. Techn. 4:399-401 (1966).

Tien, T. Y. (U. of Michigan), F. A. Hummel, L. E. Cross. "Dielectric Relaxation in Strontium Titanate Solid Solutions Containing Mixed Cations." Jap. J. Appl. Phys. 6:(3):7 (1967).

Toole, J. M., H. K. Henisch, K. Miyashita. "Thermo-Voltaic Radiation Dosimetry." Nature 213:698-699 (1967).

Vand, V., J. I. Hanoka. "Epitaxial Theory of Polytypism; Observations on the Growth of PbI_2 Crystals." Mat. Res. Bull. 2:241-251 (1967).

Vand, V., G. G. Johnson Jr "Generalized Methods of Indexing X-ray Powder Patterns." Materials Research Laboratory Publication, PSU, 33 pp. (1967).

Vand, V., K. Vedam. R. Stein. "The Laser as a Light Source for Ultramicroscopy and Light Scattering by Imperfections in Crystals. Investigation of Imperfections in LiF, MgO, and Ruby." J. Appl. Phys. 37:2551-2557 (1966).

Vastola, F. J., A. J. Pirone, B. E. Knox. "The Production of Vapor Species in a Mass Spectrometer Ionization Chamber." Proc. 14th Ann. Conf. on Mass Spectrometry (Pittsburgh, Pa.), p. 78 (1966).

Vedam, K., E. D. D. Schmidt. "Variation of Refractive Index of MgO with Pressure to 7 Kbars." Phys. Rev. 146:548-559 (1966).

"Nonlinear Piezooptic Behavior of Sphalerite (α-ZnS)." Phys. Rev. 150:766-767 (1966).

"Piezooptic Behavior of RbCl up to the Phase Transition Point." J. Mat. Sci. 1:310-311 (1966).

Vedam., K., D. L. Miller, R. Roy. "Elastic Constants of Selenium in the Hexagonal and Glassy Phases." J. Appl. Phys. 37:3432-3434 (1966).

Vedam, K., E. D. D. Schmidt, R.Roy. "Nonlinear Variation of the Refractive Index of Vitreous Silica with Pressure to 7 Kbars." J. Am. Ceram. Soc. 56:1741-1742 (1966).

Walker, P. L., Jr., Y. Sasaki. "Effect of Oxygen Chemisorption on the Thermoelectric Power of Carbon and Graphite Artifacts." Carbon 4:536-538 (1966).

Walker, P. L., Jr., M. Shelef. "Carbon Dioxide Sorption on Carbon Molecular Sieves." Carbon 5:7-11 (1967).

Walker, P. L., Jr., A. Weinstein. "Carbon Produced from Known Organic Compounds. I. Anthracene and Phenanthrene." Carbon 5:13-17 (1967).

Walker, P. L., Jr., L. G. Austin, S. P. Nandi. "Activated Diffusion of Gases in Solids." Fuel 45:173-175 (1966).

"Activated Diffusion of Gases in Molecular-Sieve Materials." Chem. Phys. Carbon 2:257-371 (1966), Marcel Dekker. N. Y.

Walker, P. L., Jr., T. C. Lamond, J. E. Metcalfe, III. "The Preparation of 4A and 5A Carbon Molecular Sieves." Second Industrial Carbon and Graphite Conference (London), pp. 7-14 (1966).

Walker, P. L., Jr., W. O. Stacy, E. Wege. "Carbon Bodies Prepared from Demineralized Anthracite - A Comparative Study with Delayed Petroleum Coke." Carbon 4:129-135 (1966).

Weber, J. N. "Bibliography - Geochemistry of the Stable Isotopes of Carbon and Oxygen." 2nd Monograph 1, Materials Research Laboratory, PSU, 125pp. (1967).

Weber, J. N., D. M. Raup. "Fractionation of the Stable Isotopes of Carbon and Oxygen in Marine Calcareous Organisms - The Echinoidea. Part I. Variation of C_{13} and O_{18} Content within Individuals." Geochim. Cosmochim. Acta 30:681-703 (1966).

"Fractionation of the Stable Isotopes of Carbon and Oxygen in Marine Calcareous Organisms - The Echinoidea. Part II. Environmental and Genetic Factors." Geochim. Cosmochim. Acta 30:705-736 (1966).

Weber, J. N., R. T. Greer, V. Vand. "Electron Excited Fluorescence of Serpentines." Planetary Space Sci. 15:633-643 (1967).

White, E. W., H. A. McKinstry. "Chemical Effects on X-Ray Absorption Edge Fine Structure." Advances in X-Ray Analysis, pp. 376-392. Ed. Mallay, Ray and Mueller, Plenum Press (1966).

White, E. W., R. Roy. "Use of X-Ray Emission Spectroscopy in the Characterization of Thin Films of Aluminum Oxides and Hydroxides." Mat. Res. Bull. 2:395-398 (1967).

White, E. W., G. V. Gibbs, G. G. Johnson Jr., G. R. Zechman Jr. "X-Ray Wavelengths and Crystal Interchange Settings for Wavelength Geared Curved Crystal Spectrometers" (2nd Edition). Mineral Industries Experiment Station Special Pub. No. 3-64, PSU, 195 pp. (1965).

"Supplement to X-Ray Wavelengths and Crystal Interchange Settings for Wavelength Geared Curved Crystal Spectrometers." PSU, 66 pp. (1966).

White, W. B. "Application of Infrared Spectroscopy to Order-Disorder Problems in Simple Ionic Solids." Mat. Res. Bull. 2:381-394 (1967).

White, W. B., B. A. D'Angelis. "Interpretation of the Vibrational Spectra of Spinels." Spectrochim. Acta 23A:985-995 (1967).

White, W. B., K. L. Keester. "Optical Absorption Spectra of Iron in the Rock-Forming Silicates." Am. Mineral. 51:774-791 (1966).

White, W. B., V. A. Schmidt. "Hydrology of a Karst Area in East-Central West Virginia." Water Resources Res. 2:549-560 (1966).

1.2.8 Agencies Supporting Research

Department of the Air Force:

Wright-Patterson Air Force Base, Systems Engineering Group

Air Force Office of Scientific Research: Solid State Sciences Division

Department of the Army:

Defense Supply Service - Washington, Advanced Research Projects Agency

U. S. Army Electronics Command

U. S. Army Engineer Research and Development Laboratories

U. S. Army Materials Research Agency

U. S. Atomic Energy Commission:

Division of Biology and Medicine

Metallurgy and Materials Program

National Aeronautics and Space Administration:

Sub-grants under NASA Institutional Grant

Goddard Space Flight Center, Thermal Systems Branch, Spacecraft Tech. Div.

National Science Foundation:

Engineering Materials, Engineering Division

Geochemistry, Earth Science Division

Mathematical and Physical Sciences, Earth Science Division

Office of Naval Research:

Metallurgy Branch

Public Health Service:

National Institute of General Medical Sciences

National Institute of Arthritis and Metabolic Diseases

2.0 RESEARCH RESULTS: Material Preparation

2.1 Growth of "Large" Crystals

2.1.1 Flux Method

2.1.1.1 Growth of Calcite

(J. F. Balascio, W. B. White, R. Roy)

Calcite has been grown from a Li_2CO_3 flux in a hydrothermal pressure vessel with a pressure of 700 psi of CO_2 to prevent the decomposition of $CaCO_3$. The cooling rate was 3°C per hour with a weight percent of $CaCO_3$ ranging from 64% to 50%. The crystals obtained were ~1mm in size and a diffractometer powder pattern indicated the correct lattice parameters. Unfortunately, Nester and Schroeder of Perkin-Elmer Corporation have just published very similar results and therefore this approach has been suspended for the time being.

Current work has shifted to flux methods with the following compositions:

(1) $CaCO_3$-$Ca(NO_3)_2$

(2) $CaCO_3$-$NaNO_3$

2.1.2 Hydrothermal Growth

GeO_2 and SiO_2 (R. Roy and S. Theokritoff)

This study is aimed chiefly at establishing the feasibility of growing large crystals of a phase where it is thermodynamically metastable. Melt techniques would seem to be least favorable both because of the higher temperatures and the high concentrations. Vapor phase and especially hydrothermal techniques commend themselves. Because of our past experience with the hydrothermal growth of GeO_2 in the rutile form, it was decided to place the greatest emphasis on growth of GeO_2 in the quartz form, which is metastable throughout the 'hydrothermal range.'

The nutrient material used throughout has been vitreous GeO_2. A wide range of p-t conditions has been tried, and also a wide range of temperature differentials between nutrient and "seed" if any. The main hope has lain on epitaxial nucleation and growth on a suitable substrate. SiO_2-quartz has been the chief substrate material used so far. Different crystallographic directions as well have been tried for the quartz-SiO_2 seed plate, using at first crystals cut parallel to the minor rhomb face, and later the z-cut (0001) face, which has a much smaller mis-match in lattice spacing compared with quartz-GeO_2 than have other crystallographic directions. Some $AlPO_4$ crystals have also been used since its lattice spacings are also much closer to those of GeO_2. Finally some comparisons have been made using GeO_2 rutile substrates to check whether solubility and gradient conditions were appropriate for growth of even the stable phase.

Small gains in the seed crystal weight have been observed under various experimental conditions, but the proper sets of conditions have not as yet been achieved for extensive growth on the seed crystals used. Quartz-GeO_2 has, however, been recently successfully grown metastably by spontaneous nucleation and this gives grounds for hope that this growth process can be worked out systematically in the near future.

2.1.2.2 Sphalerite-Wurtzite Stability Relations

(S. D. Scott and H. L. Barnes)

In the last annual report, the univariant nature of the sphalerite (sulfur rich)-wurtzite (sulfur deficient) phase change as a function of f_{S_2} and temperature was demonstrated by hydrothermal and dry gas experiments. Since then, the hydrothermal experiments in concentrated NaOH solutions have been extended to 700°C. Sphalerite reappears as the stable

phase along with acicular Na_2SO_4 crystals at about 570°C in 6.2m, 600°C in 10m, and 700°C in 15m NaOH. Thus for a given solution there is a phase change from sphalerite to wurtzite and then back to sphalerite with increasing temperature. The reoccurrence of sphalerite above 600°C is undoubtably due to the interference of Na_2SO_4. The hydroxyl ion activity in the NaOH solutions is lowered resulting in the precipitation of sulfur-rich zinc sulfide which is sphalerite. This also means that any attempts to control zinc sulfide compositions within the stability field of Na_2SO_4 will be successful.

Excellent growth of sphalerite single crystals has been obtained in 5m NH_4I solutions between 400 and 600°C. Carbon is added to the charge to act as an oxygen buffer to prevent corrosion of the gold tubes. In runs in which no buffer was present, large (up to 2mm.) platey single crystals of gold were grown. In addition, the sphalerite crystals (also up to 2mm. diameter) had a distinct purple color.

Several attempts have been made to measure directly the univariant f_{S_2}-temperature relationship for coexisting sphalerite and wurtzite between 500° and 600°C by buffered experiments using pyrrhotite ($Fe_{1-x}S$) as an f_{S_2} indicator in aqueous NH_4I solutions. The pyrrhotite and zinc sulfides are separated by thin-walled platinum tubing which allows f_{H_2} (hence f_{S_2}) equilibration without contaminating the ZnS with iron. In every run, however, f_{O_2} was high resulting in larger values of f_{S_2} than required for sphalerite-wurtzite equilibrium. Efforts are being made to overcome this by buffering f_{O_2} and controlling pH.

Direct measurements of f_{S_2} along the sphalerite-wurtzite boundary have been made at high temperatures and 1 atm. pressure by passing calibrated H_2/H_2S gas mixtures over ZnS powders. The two zinc sulfides coexist at an

f_{S_2} of 10^{-5} at 890°C and about $10^{-7.5}$ at 700°C. Reaction rates are extremely slow so that equilibrium is difficult to attain, especially near the univariant boundary.

This work on the effect of stoichiometry on the inversion temperature of ZnS is nearly completed and will soon appear in the Ph.D. thesis of S. D. Scott. In October 1967 we will begin to extend this concept to other sulfide pairs such as HgS (cinnabar and metacinnabar), FeS_2 (pyrite and marcasite), and Ag_2S (argentite and acanthite).

2.1.2.3 Hydrothermal Growth of HgS Crystals

(S. D. Scott and H. L. Barnes)

In the last annual report, a method of growing mercury sulfide (cinnabar) crystals on a cold finger inserted into a rocking hydrothermal pressure vessel was described. The results of several runs in NaHS solutions are listed below:

Table I

Run	Molality NaHS	pH	Temperature, °C Solution	Finger	Duration (days)	Results
M-11	3.7	8	150	27	7	Thick coating of 1mm long crystals
M-12	3.7	8	70	26	12-1/2	Same as M-11.
M-13	3.7	8	165	155	11	About the same as M-11 and M-12 but crystals are somewhat smaller.
M-14	1.0	7	135	120	26	No crystal growth

The pH's and temperature gradients were chosen on the basis of solubility data for HgS in $NaOH-H_2S-H_2O$ solutions (Romberger et al., in preparation). In runs M-11, 12, and 13 a large yield was obtained but spontaneous nucleation prevented the growth of large single crystals. Since different temperature gradients had very little effect, an attempt was made in run M-14 to reduce the nucleation rate by lowering the solubility of HgS. At pH 7, HgS solubility is roughly proportional to the square of the bisulfide activity. Since no crystals were obtained in run M-14, it is apparent that the fourteen-fold reduction in HgS solubility was too severe.

The apparatus used in this research will not be available again until September, 1967. At that time, a seed technique will be used in an attempt to grow large single crystals.

2.1.2.4 Polytypism of Hexagonal Zinc Sulfide (wurtzite)

(S. D. Scott and H. L. Barnes)

In previous annual reports, the hydrothermal growth of wurtzite crystals between 470° and 700°C at 1/2 kilobar pressure in concentrated NaOH solutions was described. Two polytypes, 6H and 4H, have been identified by single crystal precession methods. Calculated and observed structural amplitudes for 00ℓ and $h0\ell$ reflections are in good agreement for both polytypes. All photos show considerable diffuse streaking, probably due to stacking disorder.

The two polytypes coexist in univariant equilibrium as a function of f_{S_2} (controlled by the aqueous solution) and temperature at 553 ± 2°C in 15m NaOH and 565 ± 2°C in 6.2m NaOH with 4H stable at higher temperatures. Preliminary calculations indicate a change in log f_{S_2} of 0.3 atm. over this temperature range.

These experiments provide evidence that wurtzite polytypes are separate thermodynamic phases with slight differences in composition. The 4H polytype is sulfur deficient (or zinc rich) relative to 6H which in turn is sulfur deficient relative to sphalerite (cubic ZnS). The composition difference between these polytypes is probably on the order of a few hundredths of an atom percent sulfur or zinc. Presumably other polytypes will be found when the right f_{S_2} and temperature conditions are achieved in the hydrothermal systems.

Polytypism controlled by stoichiometry was not considered in earlier theories. Phase changes between polytypes are first order although the free energy difference must be very small. This is indicated by the lack of an observable two phase field and the ease with which one polytype can be overgrown on another by changing f_{S_2} and temperature. Furthermore, the overgrowths indicate that although screw dislocations may perpetuate a structure, they do not initiate it and their Burgers vector can easily be changed by varying f_{S_2} and temperature. It is quite likely that polytypism in other substances such as SiC, PbI_2, and CdI_2 is also controlled by stoichiometry and temperature.

2.1.3 Growth From Melt

2.1.3.1 Growth of Crystals by Arc Fusion

(L. Brown and W. B. White)

Fusion experiments on MgO have continued with difficulties still being encountered in obtaining a large homogenous melt. The power supply is currently being modified to experiment with AC arcs which should reduce the amount of vapor present in the melt from electrolysis of the molten MgO. Spectrographic analyses have been obtained on the MgO crystals grown

so far. Impurities at about 100 ppm level are Ca, Al, Fe, and Si; all presumably present in the starting materials.

2.1.4 Traveling Solvent Method

2.1.4.1 Chalcogenide Growth

(R. W. Hamaker and W. B. White)

Preliminary zone migration experiments have been conducted using {0001} surfaces of αCdS as seed substrates and polycrystalline ZnSe as feed material. Three different materials (In, Sn and Pb) have been used as zone solvents in this work. Both the In and Sn appear to wet the ZnSe-CdS configurations uniformly below 400°C; whereas Pb does not wet the configuration uniformly until a zone temperature of about 500°C is reached. Evaporation from the zones becomes important above 600°C and does not appear to be strongly dependent on the zone metal being used. Because of the evaporation problem, zone migration runs have been attempted at 600°C for periods as long as one day. No noticeable migration has been observed at this temperature level. By utilizing enclosed silica capsule configurations, it is hoped to minimize the evaporation and increase zone temperatures until reasonable migration velocities are obtained.

Temperature gradients have been measured along the CdS seed substrates in several of the migration experiments. Values ranging from 300 to 350°C/cm have been obtained for the various metals used as solvents. Since the thermal conductivity of any of the individual solvent zones obtained by using either In, Sr or Pb can be expected to be only slightly larger than that of αCdS within the temperature range considered (i.e., 600° - 900°C), reasonable temperature gradients should be available across the zones to provide adequate driving forces for zone migration.

2.1.5 Vapor Growth

2.1.5.1 Growth of Oxides by Halide Vapor Hydrolysis

(V. Caslavaka, R. Roy)

A literature study was made of the thermodynamic properties of halides and sulfides of germanium, chromium, tin and manganese for the purpose of using these as starting materials for the vapor growth of single crystals of oxide which have the rutile type structure. The first experiments involved growing SnO_2 on rutile. The rutile was grown and prepared for the substrate. Substrate temperature from 450 to 600°C were investigated. The hydrolysis of stannic oxide was carried out at temperatures from 60 to 145°C. Thus far, the SnO_2 layers have been tetragonal and polycrystalline in nature. The substrate temperature seems to be very critical. Several NiO single crystal layers were prepared in the apparatus for the investigation of physical properties in other laboratories. Preliminary experiments to form GeO_2 layers were carried out on a rutile substrate by the hydrolysis of Germanium disulfide.

2.1.5.2 Growth of Pure Magnesium

(S. Hayden, J. W. Faust Jr.)

Large single crystals of pure magnesium had been requested by another department. A special growth furnace has been constructed for vapor growth of magnesium and other materials. The magnesium will be grown in a Ta tube placed inside of a quartz tube that is attached to a high vacuum system with cold traps. Pressures of 10^{-6} mm have been easily obtained. The quartz tube is placed inside a tube furnace. Great care was given to obtaining the proper temperature gradient in the tube. After the magnesium has been grown the apparatus will be used in a fundamental study of vapor

growth of magnesium to determine the growth forms and purity obtained under different conditions of temperature, temperature gradients and vacuum.

2.1.6 Nucleation Studies

2.1.6.1 Studies in the System PbS-PbTe

(M. S. Darrow, W. B. White, R. Roy)

Attempts to grow single crystals of solid solutions of PbS and PbTe by Bridgman and traveling heater techniques, as described in the last report, have not been successful.

Current work has consisted of measuring the variation in microhardness of polycrystalline solid solutions as a function of composition. Three different types of samples were tested: (1) mixed powders of the end members, annealed in the one crystalline phase region, (2) the same, but heated above the liquidus before annealing, and (3) oriented single crystals of the end member compounds. The solid solutions were prepared in evacuated silica tubes, some with a graphite crucible insert liner. Hardness measurements were taken on a Leitz Miniload hardness tester at loads of 50 and 25 grams.

The averaged results of ten identations per sample of Vickers microhardness values as a function of composition are given in Fig. 1. Values for the (100) and (111) faces of the single crystals of PbS and PbTe imply the existance of an orientation effect. This, coupled with the lack of solid solution single crystals, is reflected in the rather large range of value for samples of intermediate composition, but the spread was reduced when the samples were melted prior to annealing.

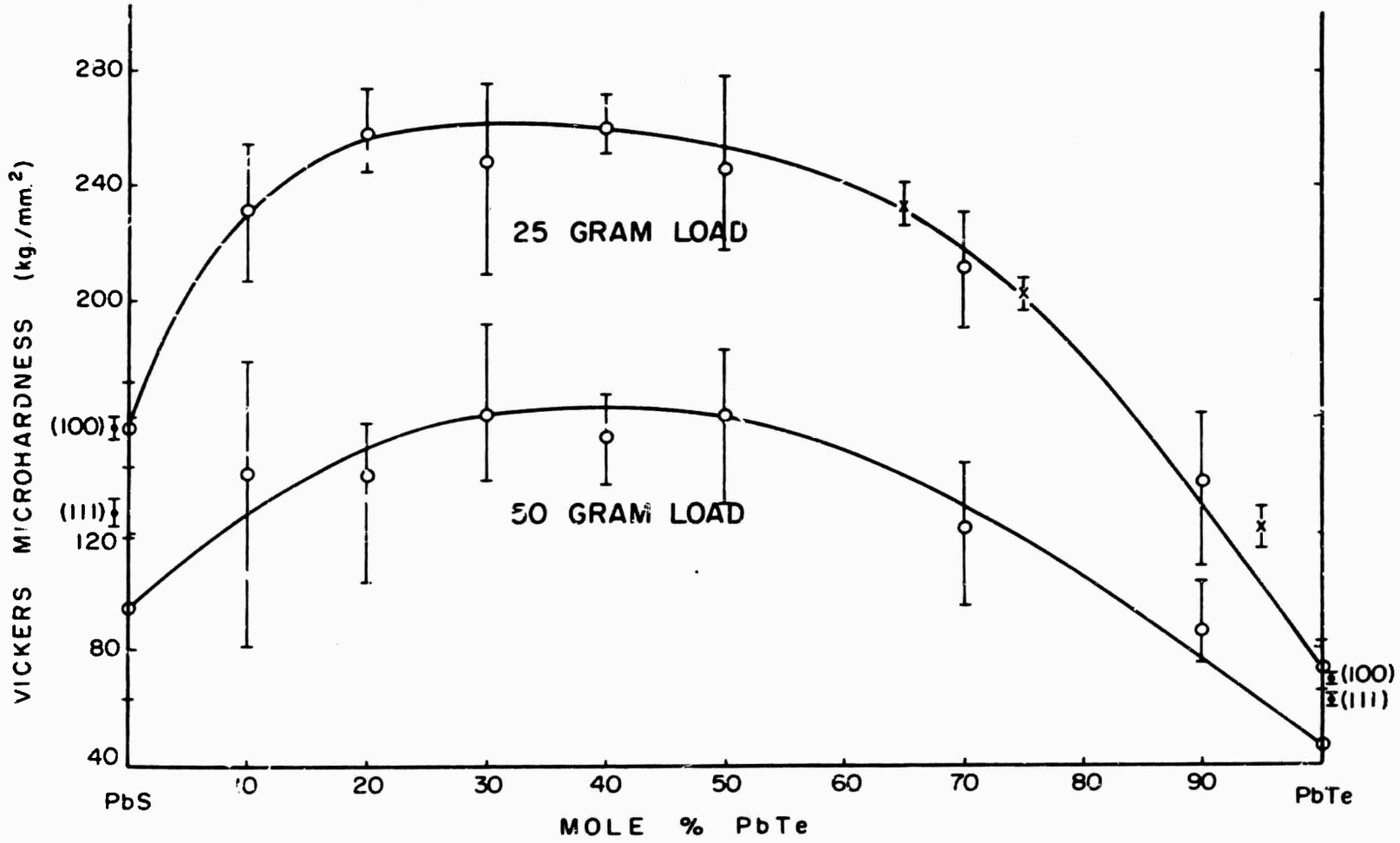

Figure 1: AVERAGE OF TEN MEASUREMENTS PER SAMPLE

⊙ Polycrystalline, annealed at 850°C (24 hrs.)

X Polycrystalline, melted at 950°C, annealed at 850°C (24 hrs.)

• Oriented single crystals (25 gram load)

I Range of ten measurements

Load time: Approximately 8 seconds full load

Despite this liability of non-ideal materials, however, there appears to be a consistent trend, with the hardness values going through a maximum value at 30 to 40 mole percent PbTe. It should be noted that the shape of this curve is quite similar to the asymmetric exsolution dome in the phase diagram, which also has a maximum at about 30% PbTe. This may mean that the increase in hardness is due to some precipitation during quenching, rather than being an intrinsic property of the solid solution. Additional measurements will be made on samples quenched from different temperatures, and attempts will be made to correlate the results with electron micrographs of the samples. Measurements will also be made on solid solutions of PbS and PbSe, where no exsolution appears in the phase diagram, and compared to the PbS-PbTe system.

2.1.3.2 Nucleation studies in network-forming liquids

(J. S. Berkes and W. B. White)

Solution behavior in Alkali Borate - NiO systems

The liquidus for the binary joins $K_2B_4O_7$-NiO and $Rb_2B_4O_7$-NiO were re-refined and quantitatively analyzed in terms of the type of solution behavior exhibited. It was found that the above two systems, as well as the system $Na_2B_4O_7$-NiO, exhibit nearly "ideal" solution behavior.

The experimentally determined liquidus for the system $K_2B_4O_7$-NiO has a standard error of estimate S(N, T) of 0.25 mole % NiO (ternary composition) with respect to a liquidus calculated assuming ideal behavior, For the $Rb_2B_4O_7$-NiO system the standard error of estimate is 0.69 mole % NiO (ternary composition). The discrepancy between theory and experiment is accommodated by a statistical term which is a function of the atomic arrangement and the interatomic forces in the liquidus.

It is indeed a fortuitous accident that the deviation from ideality in these systems is very small, since this indicates that the interatomic forces should be identical between different species and that the coordination of each of these species should be the same. This condition is nowhere approached in these systems. The statistical term, which has the form

$$\frac{1}{2} N \sum_{i}^{n} \sum_{j}^{n} X_i Z_i X_j E_{ij} = 0$$

X_i - fraction of component i

X_j - fraction of component j

Z_i - coordination of ith component

E_{ij} - interatomic bonding strength between ith and jth component

N - total number of atoms present

n - number of distinct species present

is nearly zero by coincidence and these so called "ideal" solutions are so only by virtue of the definition of ideal solution behavior.

In obtaining a best fit, for an equation of the experimental liquidus, it was found that the statistical term should be a quadratic in composition and temperature.

Nucleation Kinetics

The only observation reportable to date on the nucleation kinetics is that in the system $Na_2B_4O_7$-NiO a supersaturation of 5°C was observed with quench times of up to 2 1/2 hr. This indicates that nucleation in this system is not of the homogeneous variety unless the energy required for the homogeneous nucleation of NiO is extremely small.

System B_2O_3-NiO

The compound $3NiO \cdot B_2O_3$ was found to be stable below 1330 ± 5°C. Above that temperature it dissociates into NiO and $NiO \cdot B_2O_3$. The 1:1 nickel borate, which has not previously been reported in the literature is unstable below 1303 ± 5°C and appears to be stable up to approximately 1470°C.

2.2 New Growth Techniques

2.2.1 Growth of Concentrated Crystalline Solutions: Rare Earth Vapor Deposition, Oxidation, and Subsequent High Temperature Diffusion Studies with MgO Substrates

(L. Murr and R. Roy)

This study, which concerns itself in the main with the formation of rare earth oxide solutions in MgO host crystals, has involved the following: (1) A special ultra-high vacuum unit was initially designed and constructed for the vapor deposition of rare earth metals onto MgO substrates. The system has functioned quite routinely at pressures of 10^{-9} torr. Erbium is the rare earth metal presently of interest. (2) During the examination of erbium metal foils initially vapor deposited onto NaCl (100) substrates, transmission electron microscopy revealed several striking features of this system. Tiny crystals in (100), (110), and (111) orientation were observed to have grown in the erbium thin films; and subsequent analysis of these crystals by selected area electron diffraction and electron microprobe X-ray microanalysis has indicated the crystals to be the divalent erbium oxide, ErO. A unique feature of these crystals, particularly in (100) orientation is the formation of a twinned system on exposure to the electron beam. (3) Further electron microscopy analysis of pure erbium foils directly within the electron microscope revealed that

the erbium foil could be recrystallized and simultaneously oxidized in situ. A rigorous electron transmission and diffraction microscopy analysis of erbium oxidation and subsequent Er_2O_3 recrystallization and grain growth has been completed. The trivalent erbium oxide "film" in the terminal grain growth state has been unambiquously identified as having the bcc structure. This work is unique in that it will allow certain theoretical grain growth properties to be investigated directly, and their validity unambiguously confirmed or rejected. A computer program has been written to be used jointly with direct electron transmission analysis of the geometrical properties of equilibrated grain boundaries in the regrown oxide film. In this way, it will be possible to statistically evaluate grain boundary equilibration, to evaluate the statistical spread of equilibrated grain boundary energy ratios, and to compare these results directly with equivalent results which would be obtained by a simple 2-dimensional analysis of grain growth features by optical surface microscopy or related surface methods. This technique is unique since it represents the first application of 3-dimensional structural analysis of grain boundary geometries and energies in a ceramic-type material; as opposed to metallic systems as developed by the author. (4) Several MgO crystals measuring 5 x 5 x 0.5mm nominal size with 2.5 micron layers of Er per side have been prepared, and a third crystal of the same thickness measuring about 1cm on an edge has one side vapor deposited with 2.5 microns of Er. These crystals will be subsequently oxidized and held at high temperature for the final diffusion process. From the fundamental oxidation processes revealed by electron microscopy, it has been determined that Er can probably be completely oxidized in air at approximately 700°C after a few hours. Subsequent diffusion following complete oxidation will be carried out at 1400°C for

periods estimated at 10-30 hours. Estimates of the rare earth oxide solution concentration in the present crystal preparations are approximately 2-3%.

2.2.2 Crystal Growth in Gels

(H. K. Henisch, E. S. Halberstadt, J. Dennis, A. Dugan)

Crystal growth in gels has been explored from two general points of view in order to obtain better and more general understanding of the process than is now available.

(1) A survey has been made of a large number of "insoluble" inorganic compounds in order to find out what type of compound could be expected to yield sizable crystals in gels. As a result of this survey, about a dozen materials have been grown as small single crystals, some of good shape, others as needles. The substances grown include barium chromate, barium sulphate, barium selenate, lead chromate and lead sulphate in 2 forms, lead thiosulphate, potassium cobaltnitrite, silver chromate (or dichromate) and thallium iodate. Any of these processes would be worth further investigation, with a view to optimizing the systems for the production of larger crystals, if such crystals were needed.

A tentative conclusion can be drawn from the survey which does not yet include metals. It is that the main factor which determines whether single crystals are easily obtainable is whether a system easily forms collodial precipitates or not, the tendency to form such precipitates being always undesirable. The next step should be to find conditions which impede the production of colloidal particles and would hence allow us to grow interesting compounds like sulphides of the group IV elements which have so far presented difficulties.

(2) A parallel investigation of the gelling mechanism has been in progress. It should help us to understand the nature of the processes which go on in the gel and its function in the growth system. A gelling mixture was examined under the laser ultra-microscope, capable of showing up nuclei of 600-800Å size. These particles were streaming slowly, showing the presence of convection currents. After gelling, similar particles were still visible but were at rest, endorsing our conclusion that there are indeed no macroscopic convection currents after gel formation.

It has been clear for some time that the suppression or, at any rate, immobilization of nuclei is one of the principal functions of the gel. The question is how this immobilization is achieved. One possibility is that a foreign nucleus on which crystallization might otherwise take place finds itself surrounded by gel-matter in a closed cell too small to provide access to any appreciable amount of solute. Another possibility is that foreign nuclei might actually be involved in the initiation of the gelling process and might be held in the gel structure by chemical bonds. In an attempt to resolve this point, a number of gels were gelled in the presence of deliberate additions of foreign nuclei (fine rutile powder and graphite) in varying concentration. It was found that the foreign particles did not affect the speed of gelling in any appreciable way but do affect the number of crystals eventually formed. The first of the two models is thus more likely to be correct. Experiments on the effect which ionic impurities have on gelling and on subsequent crystallization are now in preparation.

(3) The results of nucleation and growth experiments carried out in the second half of 1966 have been incorporated in a paper which has since been published: "Nucleation and Growth of Crystals in Gels" by J. Dennis and H. K. Henisch, [J. Electrochem. Soc. 114, 263 (1967)].

(4) Work has continued on the electrical and optical characterization of gel-grown PbI_2 crystals. The results have been incorporated in a paper which has been accepted for publication in the J. Phys. Chem. Solids: "Fundamental Optical Absorption and Photoconduction in PbI_2 Single Crystals" by A. E. Dugan and H. K. Henisch. It provides a good example of a case in which the exploration of a new material was made possible (or, at any rate, practicable) through the provision of gel-grown specimens.

The paper describes measurements of the optical absorption of gel-grown PbI_2 in the region from 0.5μ - 15μ and the photoconductive measurements in the region of the absorption edge at about 0.525μ. The edge is dichromatic, with a splitting of 0.048eV which is explained in terms of a split valence band. The absorption edge of PbI_2 for $E \perp c$ is found to obey Urbach's rule for $\alpha = 50cm^{-1}$ to $10^4 cm^{-1}$ in the temperature range 144°K to 361°K and has a temperature dependence which may be represented by $(\Delta E/\Delta T)_\alpha = (9.95 - 0.60 \ln\alpha) \times 10^{-4} eV/°K$. A well defined absorption band at 4.2μ and an activation energy of 0.26eV evaluated from the measurements of dark current vs. 1/T are attributed to a deviation from stoichiometry. The exciton effective mass in PbI_2 is estimated to be $M = 0.094m_o$.

2.2.3 Plasma Synthesis

(C. P. Brooks, B. E. Knox, F. J. Vastola)

Plasma synthesis of polymers is being carried out in two rather different reaction vessels; both are part of a common vacuum system. One operation consists of passing the reacting species through a long Pyrex tube over which a microwave plasma generator is passed back and forth continuously supplying dissociation energy to the gas feed. The polymer deposits on the inner walls of the glass tubing. The second unit is an

electrode type of discharge unit, in which energy is supplied to Tungsten filament electrodes via a 1000V DC power supply. The glow discharge in this unit occurs along the cathode filament and it is on this electrode that the polymer is deposited.

With reference to the microwave discharge unit two important sampling techniques have been developed. One involves the collection and preparation of the polymer material for infra-red analysis, while the second involves the sampling of the gaseous by-products of the reaction for analysis by mass spectrometry. Previous experiments with the electrode discharge unit indicated that one of the important parameters effecting the uniformity of the plasma sheath around the substrate electrode (and consequently the uniformity of the polymer coating) is the pressure of the reacting species. Therefore, the reactor has been modified to permit closer control of the pressure of the reacting species.

Present work calls for a continuation of polymer synthesis using both the microwave and electrode type of discharge technique with both hydrocarbon and silane feed materials. Characterization of all polymer samples will be carried out using one or more combinations of the following analysis: chemical analysis, infra-red spectroscopy, mass spectrometry and possibly electron spin resonance.

Experiments underway now using the electrode discharge unit includes first of all an examination of the plasma glow as a function of system voltage, current, pressure and feed gas. The main objective in using this type of plasma generation is to determine the efficacy of the technique in coating the polymer onto a substrate. The substrate functioning as the cathode in this instance. Optical microscopy will be used to examine the continuity of these polymer coatings.

3.0 RESEARCH RESULTS: Materials Characterization

3.1 Application of the Electron Microprobe to the Characterization of Solids

(E. W. White)

3.1.1 Improved Instrumentation

A new solid state readout system has been completely installed and tested. This system facilitates automatic digital readout of the various microprobe channels by means of a Model 33 Teletypewriter and tape punch. A set of Hamner (AEC Modular design) amplifiers (3), pulse height analyzers (3), ratemeters (3), scalers (3), timer (1), and programmed readout scanner (four channel) are used for X-ray intensity readout. A solid state voltage to frequency converter and specimen stage step scanner have been constructed. The voltage to frequency connecter drives one of the Hamner scalers, thus giving digital output for specimen current, electron backscatter or cathodo-luminescence intensity.

A versatile light monochromator attachment has been perfected for quantitative measurement of visible cathodo-luminescence excited in the microprobe. Figure 2 is a sketch of the attachment showing the essential components. The spectrum is "dispersed" by means of an interference filter wedge, having a linear dispersion of about 5.5 mμ/mm. The attachment replaces the ocular tube of the light microscope and allows one to either view the specimen in the normal fashion or at any desired wavelength. A set of photomultiplier tubes and slits can be interchanged for the ocular to obtain electronic readout of light spectral intensities.

3.1.2 X-ray Spectral Shift Studies

The AlK_β emission band has been recorded for a number of aluminum oxides and hydroxides including alpha and gamma Al_2O_3, diaspore, boehmite,

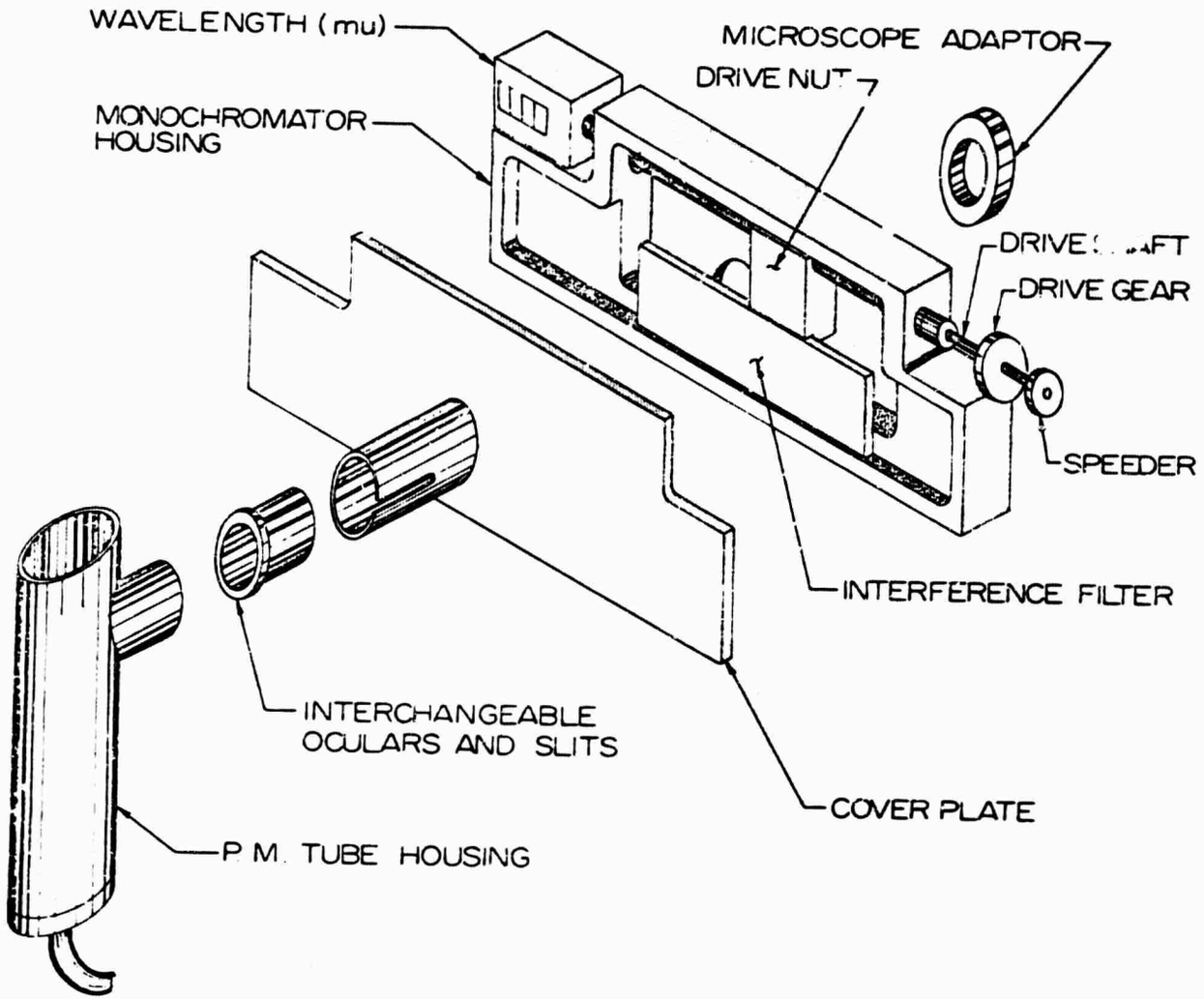

Figure 2

A Sketch of Light Monocrom Film

bayerite and gibbsite. By measuring the band shape, wavelength and intensity it is usually possible to determine which of the above phases is present in an unknown specimen. The difference between alpha and gamma Al_2O_3 is particularly striking - contrary to literature reports that claim no difference in the emission band for these two polymorphs. The emission band for the alpha phase is a distinct doublet and hence much broader than the band from gamma Al_2O_3. This marked difference in the X-ray emission band from the two polymorphs facilitates characterization of thin amorphous oxide layers such as anodized aluminum.

3.1.3 Microprobe Analysis of Trace Metals

The electron microprobe is generally not considered to be a tool for trace analysis. The typical limits of detectability are set at around 100 - 500 ppm. The reason for this limitation is the rather poor peak to background ratios that necessarily attend primary excitation of X-rays. However, if one is willing to relax requirement of spatial resolution then it is often feasible to obtain trace analysis of refractory materials by the simple expedients of operating at high specimen currents and taking replicate peak and background readings of the X-ray intensities. For example by operating at 30 KV, 0.2μA using a 15μ dia. spot size the limit of detection for Ti in an alumino-silicate matrix becomes approximately 5 ppm.

3.2 New Technique for the Study of Extended X-ray Absorption Fine Structures

(E. W. White and J. T. Hach)

A new method of obtaining extended X-ray absorption fine structure has been studied. Samples are bombarded with electrons and the continuous X-rays produced are absorbed as they pass out of the sample. The absorption

fine structure can be observed directly by measuring the X-ray spectrum at high resolution using a low take-off angle. Tests to date have been carried out by using the target areas of standard X-ray diffraction tubes as samples. For the 1-2Å wavelength region accelerating voltages of 35-50 kV, and take-off angles of 7-10 degrees appear to produce optimum resolution. The Self Absorption Fine Structure (S.A.F.S) method of obtaining spectra yields a resolution which compares favorably with that obtained by the standard thin film methods.

3.3 Instrumentation for Vacuum Path Recording of X-ray Absorption Structure

(E. W. White and W. D. Bromley)

A Seimens X-ray diffractometer and vacuum fluorescence attachment have been adapted for the measurement of X-ray absorption spectra in the wavelength range of 1 to 10Å. This has facilitated the measurement by the K-absorption spectra for Ti and V oxide compounds. In addition to the vacuum path, the temperature of the specimen can be controlled over a range from about -40°C to about 80°C so that the absorption structure can be recorded for phases which undergo transitions in this temperature range.

3.4 Instrumentation for Studies of X-ray-excited Luminescence

(E. W. White)

A light-tight X-ray fluorescence specimen chamber has been adapted for observation of X-ray excited luminescence. The monochromator described in section 3.1.1 as well as conventional grating monochromators can be used to disperse the optical spectrum. Light intensities are recorded via strip chart recorder or digitally by means of the voltage to frequency converter.

3.5 Scanning Electron Microscope

(E. W. White)

A JEOL scanning electron microscope has been installed and is currently undergoing preliminary evaluation. It appears that it will be capable of approximately 250Å resolution. It is planned that this instrument will be used extensively for the characterization of growth, etch, nucleation and fracture features for the wide variety of materials encountered in the ARPA research program.

3.6 Polytypism in PbI_2

(V. Vand and J. I. Hanoka)

The major effort of this work in the past year has been to analyze the X-ray data taken from over 650 crystals and to see how all this data might be understood in terms of the epitaxial theory of polytypism. This theory postulates that polytypism is due to screw dislocations which are formed by epitaxy around a foreign nucleus. Vand originally suggested this in 1951 and it was further discussed by Vand and Hanoka in 1967. Frank's theory of polytypism also invoked a screw dislocation mechanism but the suggested origin of the screw dislocation - a buckling and cracking to expire a ledge in a thin platelet of a basic structure such as 4H or 6H - led to a number of predictions which were contrary to experimental findings. For example, Frank's theory predicted no polytypism in PbI_2, and now about 30 polytypes of this substance are known. The epitaxial theory, on the other hand, would predict as extensive polytypism in PbI_2 as in any other polytypic substance, the only requirement being that the growth conditions are favorable for growth around a foreign nucleus.

Such a foreign nucleus as predicated by the epitaxial theory could ordinarily be of atomic dimensions and thereby difficult or impossible to find. By a rather fortuituous circumstance, large, macroscopic foreign nuclei have been found and identified for PbI_2 growing in a gel. A number of test tubes showed crystals growing along a limited length of the gel column and beyond this length, no further growth of crystals except for the very bottom of the test tube. At the test tube bottom a number of small crystals ($\sim$ 1mm) could be found which had obviously grown at a later time than the crystals in the upper part of the gel. The presence and location of these smaller crystals immediately suggested that they had grown on foreign nuclei which were large enough to settle to the bottom of the gel while the gel was still completely liquid (i.e. before gelling).

A search for these nuclei was quite successful. Near the center of many of the crystals, a tiny spot could be seen which may have been the foreign nucleus. The electron microprobe was used in order to see if the material of the foreign nucleus could be identified.

The first results of the probe were negative but it soon became clear why. The spots were seen to be, under closer examination, not on the surface of the crystal as was first suspected, but in the center of the crystal. A slicing technique which was developed to slice apart individual polytypes was used here to slice these crystals so that each slice could be individually studied under the probe. This turned out to be exactly what was needed - microprobe work indicated that an interior slice contained silver at the center of the slice. This was verified for other crystals which were sliced and examined under the probe. In each case silver was identified at the center of an interior slice. X-ray fluorescence analysis indicated that the silver came from the lead acetate used in growing the

PbI_2 crystals. "Reagent grade" lead acetate from 2 different suppliers was used in the crystal growth and both sources had the same amount of silver impurity present: 0.5% by weight. Silver was not listed as a specific impurity on the label of either supplier.

The crystals which nucleated on these silver-containing nuclei showed some other interesting features. A number of the crystals showed a large hole in the center of the crystal which apparently terminated within the crystal at the site of the foreign nucleus. Such a hole could be used to relieve the strain energy due to a large screw dislocation. Some of the crystals also exhibited spirals on their surface which were visible under the optical microscope. Many of the crystals showed a structure of 6 "arms" emanating from the nucleus. These arms were symmetrically disposed and were in the interior of the crystal and not present as a surface feature. It was possible to follow along these arms with the electron microprobe and this work showed that the arms also contain silver. The direction of these arms would correspond to the directions of fastest growth in the crystal. Apparently the silver is preferentially incorporated in the crystal along the directions of fastest growth.

It is known that epitaxy is a function of growth temperature and also growth rate. Experiments on polytypism in gel-grown PbI_2 as a function of these two growth parameters were carried out and the bulk of this work was reported in the last yearly progress report.

The number of specimens in each growth batch in these experiments was 35 in most cases. The fact that no specific, quantitative, relations could be obtained might be due to the relatively small size of the statistical sample used. A larger number of specimens for each growth batch would certainly have improved the statistics, but such experiments would have

required a formidable amount of time to complete. In lieu of this, it was decided to take all the data obtained from all the crystals studied and see if the large statistical sample obtained in this way would yield any meaningful results.

A total of 650 crystals were X-rayed in the course of all the studies performed in PbI_2 polytypes. Using all the data obtained from this large number of crystals would, of course, wash out any specific effects of concentration or temperature, but it was felt that this would not introduce any serious errors.

It was found that if the rhombohedral polytype distribution is plotted, the distribution is closely described by a Poisson distribution of the form:

$$p_s = \frac{e^{-m} m^s}{s!}$$

where p_s = probability of s occuring

m = a constant, in this case $m = 12$

$s = 6n$, $n = 1, 2, 3, \ldots$

The curve has a maximum at 12R, and the next most frequently occuring polytype is 18R. The curve would imply that there is a finite but small, probability of very high polytypes occuring. The theoretical distribution would predict more of 6R than what was found. The presence of 6R in some crystals may have been masked by the presence of 12R, as the 6R polytype has reflections which are also in 12R positions.

The reason the rhombohedral polytypes in particular should obey such a distribution became clear after a detailed study of syntactic coalescence. The major result to emerge from this investigation of coalesence was a very significant connection between hexagonal and rhombohedral polytypes. It

was discovered that an nH polytype was often coalesced with a 3nR polytype. 32 examples of 4H with 12R were found, 5 examples of 6H with 18R, one example of 8H with 24R, two examples of 10H with 30R, and one example of 14H and 42R.

In the case of 10H —> 30R, additional evidence for this came from the slicing technique already mentioned. In this case, the 10H and 30R polytypes were actually sliced apart. The slicing technique was employed on a crystal which was about 1.5mm thick in the <00.1> direction. This crystal was sliced into 19 slices, each 0.08mm thick. The slices were X-rayed individually and showed the crystal to be formed of the polytypes 12H, 20H, 10H, 30R, and 2H, in order of stacking. The first interesting thing to note here is that of the 10H and 30R polytypes being adjacent. This crystal also shows that a hexagonal polytype nH does not necessarily form a 3nR above it, as is witnessed by the presence of 20H immediately above 12H and no evidence of any rhombohedral structure in between. Between the 20H and 10H, some of the crystals were irretrievably lost and the polytype present here is not known.

Some other features of this sliced crystal are noteworthy. Since it now seems established that the 30R grew over the 10H, then the 2H which was over the 30R was last to grow. This then is evidence of what was suggested by Vand and Hanoka (1967) as an explanation for those cases in which a crystal showing a higher polytype showed no surface spirals, as would be expected from a screw dislocation theory. A thin layer of 2H growing over the higher polytype would not show any spirals, or at least no spiral corresponding to the higher polytype in the bulk. The coalesence of the two hexagonal polytypes, 12H and 20H could be explained by the

incorporation of a foreign nucleus which changes the Burgers vector, as was suggested by Vand and Hanoka (1967).

The X-ray photographs of the separate slices do not indicate coalescence except for the top slice which shows 2H with 30R. This indicates that the razor blade used for the slicing always managed to notch itself in a groove which was the join between 2 different polytypes. Thus, this slicing method is capable of physically separating polytypes which are syntactically coalesced, and should be an important technique in any further work on polytypism.

The discovery of an nH —> 3nR correspondence immediately suggests how rhombohedral polytypes could form. All that would be needed is a partial dislocation $\vec{r}$ in the (00.1) plane whose Burgers vector would add to the Burgers vector $\vec{b}_{nH}$ of the nH polytype to give an inclined dislocation with a Burgers vector $\vec{b}_{3nR}$:

$$\vec{r} + \vec{b}_{nH} = \vec{b}_{3nR}$$

A three fold repetition of $\vec{b}_{3nR}$ would return everything to a similar orientation and give the hexagonal unit cell. $\vec{r}$ would be = the distance between 2 close packed positions, when projected on (00.1).

3.7 Dislocation Probe Technique for Characterization of Defects Induced by Surface Contamination and γ-irradiation

(K. Vedam)

In contrast to the vast amount of work done on the hardening effects of gamma radiation on the mechanical properties of alkali halides, little is known of similar effects in CaF_2.

When these crystals are γ-irradiated, the radiation damage induces coloration. The optical absorption spectrum of these crystals consists

of four absorption bands with peaks occurring at 580mμ, 400mμ, 335mμ and 225mμ. O'Connor and Chen[1] have attributed this absorption to the optical transitions of the Y^{2+} impurity in the crystal. In previous published reports on the growth of the color centers corresponding to the absorption peaks, an irradiation time of up to 10 hours of hard X-rays and high energy electrons was observed to cause saturation of all the four peaks after about two hours of irradiation. In the present investigation massive radiation dosages of 1.33 Mev γ-rays of up to 3×10^8 r results in a rapid growth of the center corresponding to the 335mμ peak. The remaining three peaks continue to remain saturated. The rise in the 335mμ begins at approximately 7.5×10^7r. This observation suggests that in addition to the absorption by Y^{2+} impurities, a possible new color center is generated by the γ-ray bombardment.

A study of the variation of Vicker's microhardness, dislocation mobility and flow stresses with γ-irradiation dosage suggests that the rapid change in the above mentioned mechanical properties in the high dosage region is connected with a new color center which absorbs light at 335mμ. The occurrrence of absorption of this center at the same wavelength as that due to the Y^{2+} transition cannot be explained at present and is tentatively considered to be a pure coincidence. The gradual hardening of CaF_2 in the low dosage region seems to be connected with the Y^{2+} impurities. These Y^{2+} impurities arise from the radiation induced electron capture of Y^{3+} which is always present in trace quantities in CaF_2. The rapid hardening in the high dosage region can be explained in terms of the interaction of asymmetric strain fields due to F_2^- molecular ions or the V_k center. Such centers possibly arise out of F° interstitial atoms associating with neighboring F^--ions in CaF_2.

These and the investigations on the surface embrittlement of LiF, NaF and CaF_2 described in the earlier reports, from the subject matter of a Ph.D. thesis entitled "Hardening Mechanisms in LiF, NaF and CaF_2 due to Surface Contamination and γ-irradiation" by Mr. S. R. Sashital.

(1) J. O'Connor and J. Chem. Phys. Rev. 120, 1790 (1963).

3.8 Characterization by X-ray Methods

3.8.1 Hot Pressed Magnesium Fluoride

(H. A. McKinstry and W. Stitt)

The X-ray study of hot pressed MgF_2 carried on during the past year has been completed. Results of the thermal expansion determination were reported in January and will not be repeated here.

Partial results were given previously for strain in the hot pressed material and more will be reported here. The values for strain and domain size were obtained by Warren-Averbach analysis of the X-ray lines obtained at various sample temperatures from 25 to 650°C. The peaks at 650°C were those of a well annealed strain-free material, and so were used as the standard in the strain analysis.

Table II

Results of the analysis are shown in the table.

	(110)-(220)		(101)-(303)	
Temp.	Strain	Domain Size	Strain	Domain Size
25°C	$.24 \times 10^{-3}$	1350Å	$.41 \times 10^{-3}$	2100Å
200	.24	*	.30	*
400	.24	*	.27	*

*indicates that domain size was larger than the resolution of the analysis.

It is seen that the strain present is small and decreases with temperature in a direction perpendicular to the (101) plane. In addition, the domain size increased with temperature to a value which is beyond the limit of detection (greater than $\sim$ 2500Å).

Two papers on this subject are being prepared for publication.

3.8.2 Defects and Strain in Cold Worked LiF

(H. A. McKinstry and W. Stitt)

The purpose of this investigation is to study the changes in defect type and concentration and the strain as a function of annealing temperature of an initially strained sample of LiF. Preliminary measurements have shown that lithium fluoride crushed to 325 mesh size has a large amount of X-ray line broadening which decreases continuously upon annealing at various temperatures up to 650°C. There is also a large lattice parameter change with annealing but the lattice parameter reaches a constant value at a lower temperature about 450°C.

Thus, it seems that there are two processes taking place during annealing. One causes the X-ray line broadening to decrease up to 650°C, while the other allows the lattice parameter to reach a constant value at a lower temperature. The present study will attempt to understand these effects.

The defect concentration and type will be determined from lattice parameter and density measurements, and the strain from Warren-Averbach analysis of the X-ray peaks.

3.8.3 X-ray Topographic Techniques

(H. A. McKinstry and J. W. Faust Jr.)

During the year, the Berg-Barrett camera was made available as a routine characterization tool. It was positioned on a table with a Cu tube. Toward the end of the year a new microfocus X-ray generator and a Lang camera purchased and set up in a special room. The equipment is operational. is now possible to study defects in the surfaces by Berg-Barrett and in the interior of the crystal by Lang techniques.

3.9 Structure Analysis and Crystal Physics

(R. E. Newnham)

3.9.1 Crystal Structure of Ni_3TeO_6

Polycrystalline Ni_3TeO_6 was synthesized during a search for useful dielectric and magnetic materials. Bright yellow-green ceramics were prepared by the solid state reaction.

$$6NiO + 2TeO_2 + O_2 \xrightarrow{\Delta} 2Ni_3TeO_6,$$

heating the oxides to 840°C for twelve hours in air. The compound decomposes near 1000°C. Starting materials were spectroscopically pure NiO (Johnson, Mathey & Co., Ltd.) and 99.5% grade TeO_2 (Research Organic Chemical Co.).

The Ni_3TeO_6 structure was determined from X-ray diffractometer patterns using filtered CuKα radiation. Observed intensities (peak areas) and interplanar spacings are presented in Table III. The more intense lines are similar to those of corundum, and the pattern was readily indexed on a hexagonal unit cell. After calibration with a silicon standard, the angular data gave lattice parameters a = 5.103 ± .002, c = 13.755 ± .010Å. The axial ratio c/a = 2.695 ± .003 is small for a corundum-like structure, exceeding only the value for Ti_2O_3.

The indices of all observed reflections obey the rhombohedral lattice condition: $-h + k + l = 3n$. There are no other systematic absences; thus, the possible space groups are $R\bar{3}m$, $R3m$, $R32$, $R\bar{3}$ and $R3$. Assuming the Ni_3TeO_6 structure is a derivative of corundum (space group $R\bar{3}c$), the choice is narrowed to $R32$, $R\bar{3}$ and $R3$. $R\bar{3}m$ and $R3m$ are not subgroups of $R\bar{3}c$. In the absence of any physical property measurements, the final determination rests on intensity calculations. Trial atomic positions were obtained from the corundum coordinates, distributing the three nickel atoms and one tellurium over four cation sites in the rhombohedral unit cell. Fully disordered ($R\bar{3}c$), fully ordered ($R3$), and three partially ordered ($R3c$, $R32$ and $R\bar{3}$) arrangements were considered. The $R\bar{3}c$ and $R3c$ patterns are impossible because hOl reflections with l odd are observed, violating the c glide plane extinction condition.

Intensities calculated for the fully order configuration ($R3$) compare favorably with experiment, as demonstrated in Table III. Atomic coordinates and equipoints are listed below. $R32$ and $R\bar{3}$ give poor agreement for the reflections most sensitive to order, hOl reflections with l odd.

R3	O_I	9b (x,y,z);	x = .306, y = 0, z = .250
	O_{II}	9b (x,y,z);	x = .694, y = 0, z = .750
	Ni_I	3a (0,0,z);	z = .352
	Ni_{II}	3a (0,0,z);	z = .648
	Ni_{III}	3a (0,0,z);	z = .852
	Te	3a (0,0,z);	z = .148

The trinickel tellurate structure contains Ni^{2+} and Te^{6+} ions octahedrally coordinated to a distorted hexagonal close-packed array of oxygens. Each oxygen ion is bonded to three nickels and one tellurium, satisfying Pauling's

Table III

Comparison of observed and calculated intensities and interplanar spacings for Ni_3TeO_6

hkl	d_c	I (R3)	I_o	d_o
003	4.58	26	32	4.55
101	4.21	52	73	4.18
012	3.72	144	155	3.70
104	2.714	274	239	2.703
110	2.551	244	214	2.542
015	2.335	14	16	2.332
006	2.292	18	20	2.289
113	2.229	59	64	2.224
021	2.182	11	9	2.178
202	2.104	19	18	2.102
024	1.859	103	98	1.854
107	1.795	6	4	1.795
205	1.723	6	8	1.719
116	1.705	165	158	1.702
211	1.658	11	11	1.658
122	1.623	19	22	1.623
018	1.620	18	13	1.602
009	1.528	1	2	1.528
214	1.503	89	83	1.500
300	1.473	85	90	1.471
027	1.468	3		
125	1.428	7	10	1.428
303	1.403	6	8	1.403
208	1.357	7	10	1.357
1,0,10	1.313	36	56	1.313
119	1.311	28	30	1.275
220	1.276	25		
217	1.273	15		
306	1.239	18	22	1.239
223	1.229	6	7	1.229
131	1.221	4	5	1.220
312	1.207	9	15	1.206
0,1,11	1.203	2	12	1.198
128	1.198	10		
0,2,10	1.168	20	21	1.168
134	1.155	27	27	1.115
0,0,12	1.146	2	3	1.146
315	1.120	3	7	1.120
226	1.115	31	31	1.115

electrostatic valence rule. Cation ordering in Ni_3TeO_6 is contrasted with other corundum superstructures in Fig. 3. The space groups of $FeTiO_3$, $LiNbO_3$ and $Mn_4Nb_2O_9$ are $R\bar{3}$, R3c, and $P\bar{3}c$, respectively. Although, all three are necessarily derivatives of $R\bar{3}c$, they are not subgroups of one another, so that each represents a totally different ordering. This is not true for Ni_3TeO_6, since R3 is a subgroup of $R\bar{3}$ and R3c, as well as $R\bar{3}c$. It combines the cation layering found in ilmentite with the polar axis of lithium niobate, perhaps leading to ferrimagnetic of ferroelectric behavior. The physical properties of Ni_3TeO_6 are now under study.

3.9.2 Other Transition-metal Tellurates

Polycrystalline specimens of Cr_2TeO_6, Fe_2TeO_6, Mn_3TeO_6 and Mg_3TeO_6 have been prepared by solid-state reaction of the oxides. The chromium and iron compounds are isostructural with trirutile, as reported by Bayer. Neutron-diffraction experiments on Cr_2TeO_6, Fe_2TeO_6 and Ni_3TeO_6 are now in progress at Grenoble, in cooperation with Dr. E. F. Bertaut and co-workers.

Structure analysis of the isomorphous salts Mn_3TeO_6 and Mg_3TeO_6 are also in progress. Their powder patterns have been indexed on a rhombohedral unit cell but the structures differ from that of Ni_3TeO_6. The bimolecular cells are pseudo-cubic with a = 6.03Å, α = 90°46' for Mg_3TeO_6, and a = 6.22Å α = 90°40' for Mn_3TeO_6. No systematic absences other than the rhombohedral lattice condition were noted; the possible space groups are $R\bar{3}m$, R3m, R32, $R\bar{3}$ and R3. When indexed on the rhombohedral cell, reflections with h + k + l = 2n are the most intense. We are, therefore, pursuring the possibility that the heavy tellurium atoms occupy special positions at the origin and body center. Fourier maps are being computed to locate the lighter atoms.

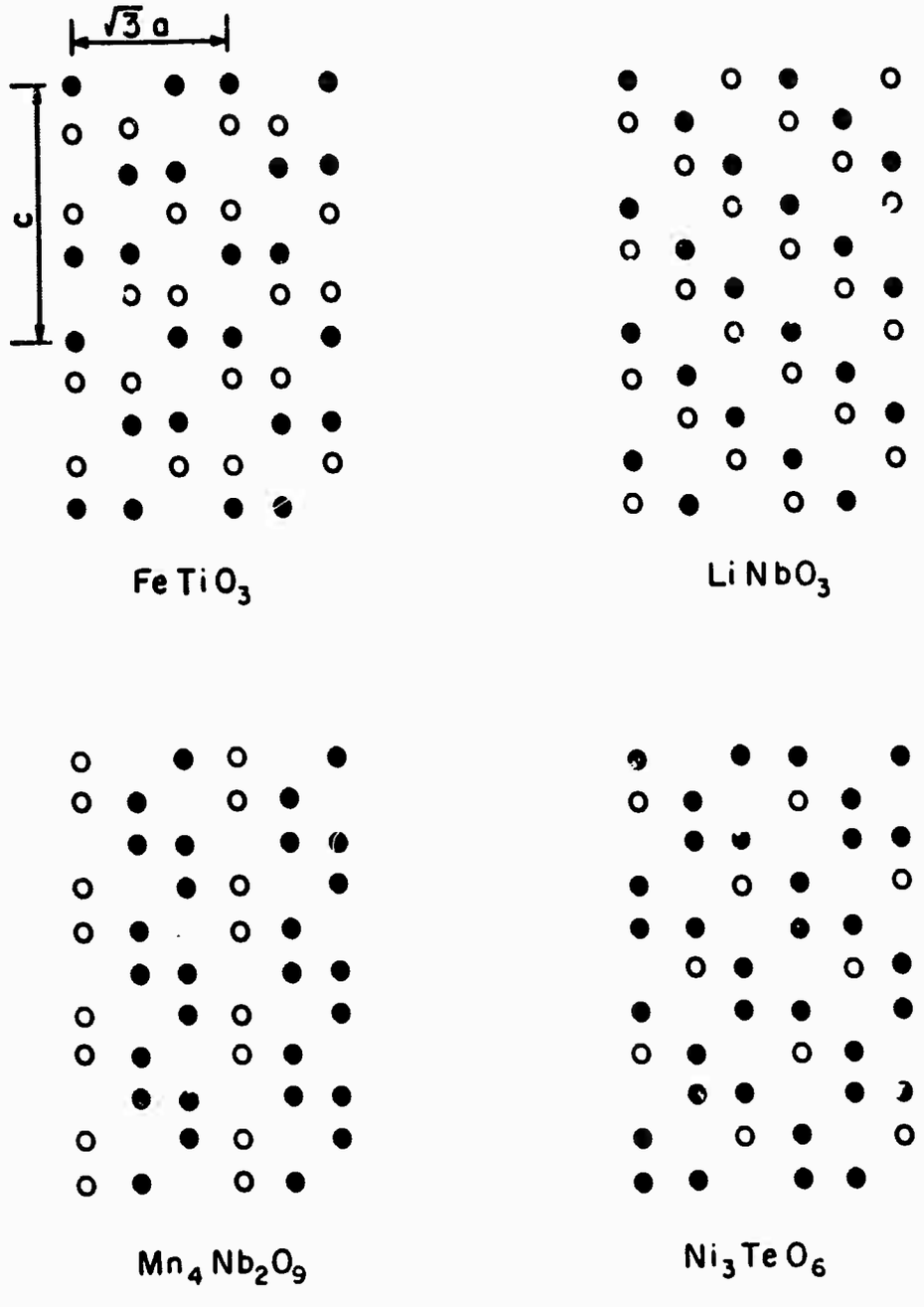

Figure 3

Four types of cation ordering based on the corundum structure

Pseudosymmetry suggests the possibility of a phase transition but none was observed in Mg_3TeO_6. Lattice parameters were computed from diffractometer patterns taken at several temperatures between 20 and 800°C. The change in $\underline{\alpha}$ was less than 2' and $\underline{a}$ showed a normal expansion coefficient of 15 x 10^{-6}/°C.

3.9.3 Crystal Structure of $ZrTiO_4$

Polycrystalline zirconium titanate was investigated during a search for high temperature dielectric materials. Capacitance bridge measurements gave an average dielectric constant of K = 37 in the 1Kc to 10Mc range. The crystal structure of $ZrTiO_4$ was determined from x-ray diffractometer patterns and refined by least squares analysis. The space group is Pbcn, orthorhombic, with a = 4.81, b = 5.45, c = 5.03Å, Z = 2. Titanium and zironium are disordered in equipoint 4c (0, v, 1/4), v = 0.300 ± 0.002, and oxygen is in general position 8d (x, y, z), x = 0.276 ± 0.011, y = 0.008, z = 0.058 ± 0.010. Oxygens form a distorted hexagonal close-packed array with metal ions occupying half the octahedral interstices. The mean (Zr, Ti)-O distance is 2.04Å.

The $ZrTiO_4$ structure (Figure 4) is isomorphous with α-PbO_2.

3.9.4 Crystal Structure and Infrared Spectrum of Pollucite

The crystal structure and infrared spectrum of pollucite were investigated as a continuation of our study of trapped molecules in silicates. Pollucite single crystals with composition $Cs_{.7}Na_{.3}AlSi_2O_6{:}0.3H_2O$ contain water molecules trapped in aluminosilicate cages. A number of H_2O molecular vibration bands, similar to those of beryl and cordierite, are observed in the near infrared spectrum (Figure 5). The principal absorption band near 2.7μ is caused by the O-H stretching vibrations. This is accompanied by

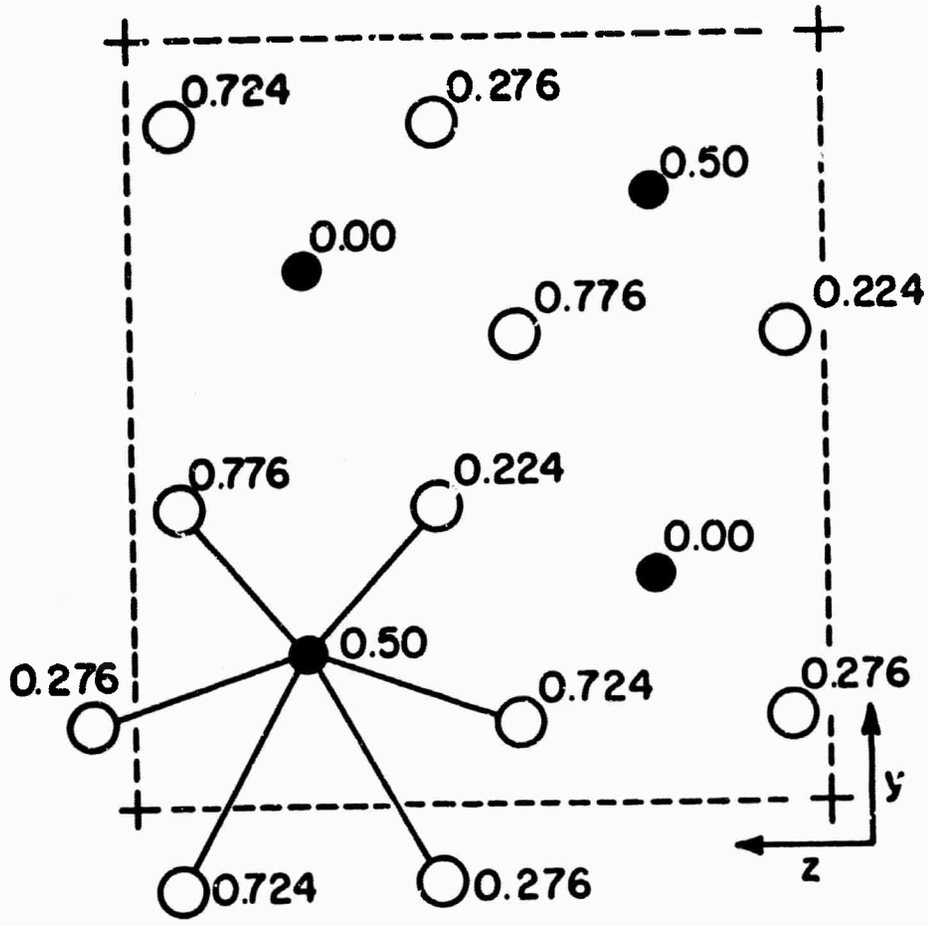

Figure 4

Crystal structure of zirconium titanate projected on (100).
Metal ions and oxygens represented by solid and open circles, respectively.

many smaller peaks at shorter wavelengths which are identified as combination bands involving the symmetric (ν_1) and unsymmetric (ν_3) stretching modes and the bending mode (ν_2). The spectrum shows a marked similarity to that of water vapor. Tentative vibrational quantum number assingments (ν_1, ν_2, ν_3) for the various excited states are listed in Figure 5. The crystal structure of pollucite has been refined by single-crystal x-ray analysis, beginning with the approximate structure proposed by Naray-Szabo. The space group is cubic, Ia3d, with a = 13.682 ± 0.003Å and Z = 16. Ten least squares cycles based on 190 observed reflections gave an R-factor of 0.13 and the following coordinates:

Cs in 16b $(\frac{1}{8}, \frac{1}{8}, \frac{1}{8})$, B = 1.7 ± 0.2.

(Al, Si) in 48g $(\frac{1}{8}, u, \frac{1}{4} - u)$, u = 0.6331 ± 0.0009, B = 0.3 ± 0.2.

O in 96h (x, y, z), x = 0.1036 ± 0.0012, y = 0.1333 ± 0.0014,

z = 0.7216 ± 0.0013, B = 1.8 ± 0.4.

From intensity calculation and crystallo-chemical arguments, we conclude that Na^+ and H_2O substitute jointly for Cs^+ in the large interstice, rather than the analcite arrangement. The mean (Si, Al)-O and Cs-O bond lengths are 1.64 and 3.48Å, respectively.

3.9.5 Magnetic and Optical Data for $CuSiO_3 \cdot H_2O$

The magnetic and optical properties of hydrous cupric silicate (dioptase) have been measured. $CuSiO_3 \cdot H_2O$ is a cyclosilicate containing Si_6O_{18} rings similar to beryl; the silicate rings are interconnected by copper atoms in square planar configuration. Magnetic susceptibility data in the paramagnetic range give $\theta = 70°K$, $\mu_{eff} = 1.86\mu_B$, and molecular field calculations predict a magnetic structure twice the size of the chemical unit cell. The diffuse

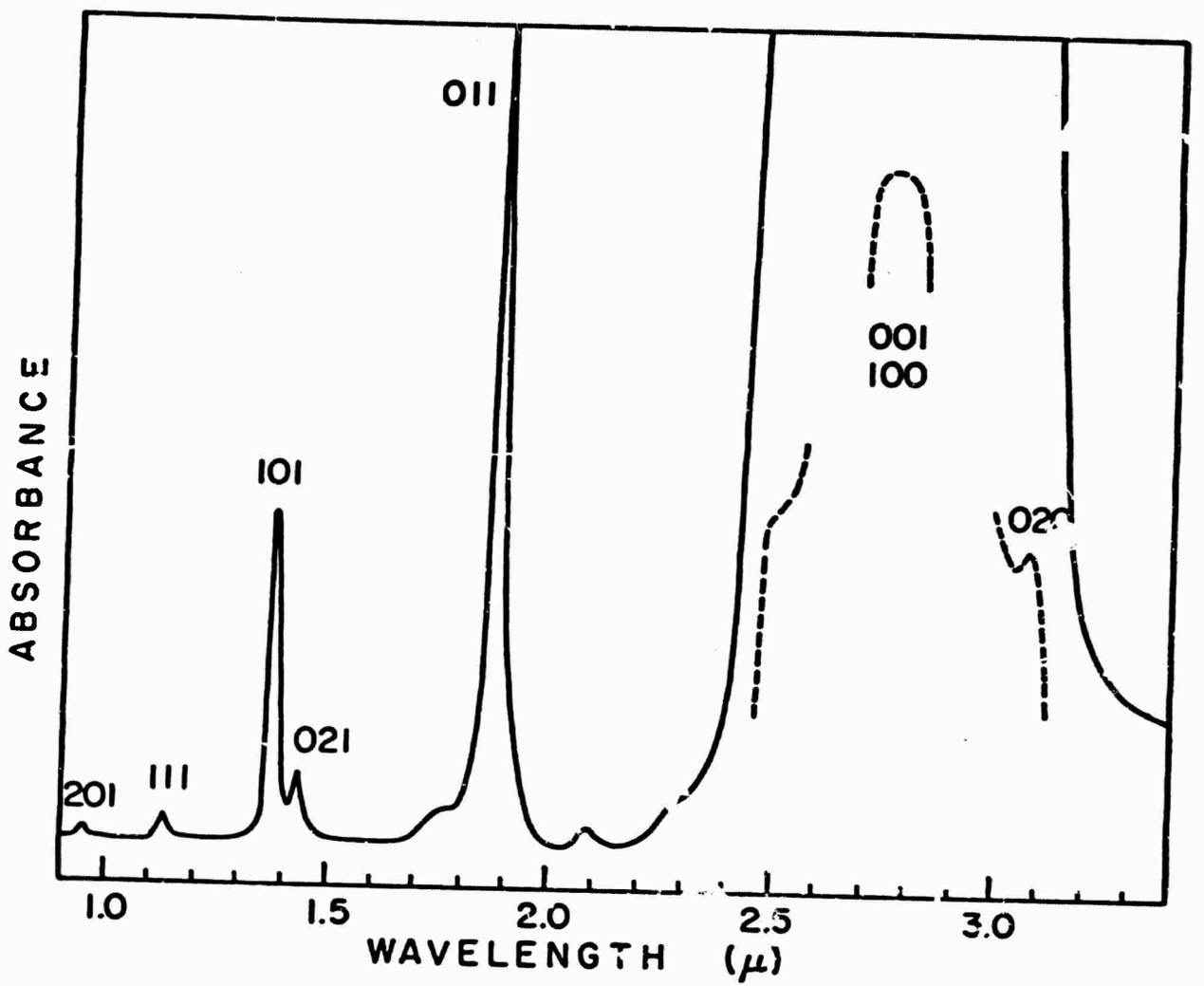

Figure 5

Near infrared absorption spectrum of pollucite

reflectance spectrum of dioptase is dominated by an intense absorption peak at 13300cm^{-1}. Based on the approximate site symmetry C4v, crystal field theory predicts a B_1 —> E electric-dipole transition in this wavelength range.

3.9.6 Magnetoelectricity

A comprehensive study of magnetoelectric materials has been prepared. The magnetoelectric effect consists of two related phenomena: magnetization induced by an applied electric field and the inverse effect, polarization due to an external magnetic field. Magnetoelectricity was first suggested by Landau and Lifshitz in 1958 and verified experimentally a year later. Our report summarizes subsequent work through June 1966. Like many physical properties, the existence of magnetoelectricity depends on symmetry; the requisite elements were predicted. Among these are the $LiMPO_4$ (M = Ni, Co, Fe, Mn) compounds we investigated earlier.

The lithium orthophosphates belong to the transition metal olivine group. Our final report on twelve of these compounds appeared during the report period. All the antiferromagnetic with Néel temperatures between 10 and 65°K.

3.10 The system, Zn-Fe-S as a Geothermomter

(S. D. Scott and H. L. Barnes)

The iron content of sphalerite in the assemblages sphalerite + pyrrhotite and sphalerite + pyrrhotite + pyrite constitutes a potentially useful geothermometer for sulfide ores. Previous work by the U.S. Geological Survey (Barton and Toulmin, 1966) done in evacuated silica tubes between 580°C and 850°C is above the range of geological interest. They present their data as contours of mole percent FeS in sphalerite as a function

of f_{S_2} and temperature which they have extrapolated to 300°C assuming ideal solution of FeS and ZnS.

In our laboratories, coexisting sphalerite + pyrrhotite and sphalerite + pyrrhotite + pyrite have been grown hydrothermally from 5m aqueous NH_4I solutions at 400-580°C and 1/2 kilobar pressure. The sphalerite crystals grow as dark brown to black tetrahedrons up to 5mm in diameter. The morphology of the pyrrhotite ($Fe_{1-x}S$) crystals varies with composition. Iron-rich pyrrhotite forms hexagonal platelets up to 5mm in diameter with a metallic luster and many surface growth features. Sulfur-rich pyrrhotite, on the other hand, grows as subhedral crystals with a very dull luster and gives broad x-ray diffraction peaks. Pyrite (FeS_2) grows as small cubes. The iron content of sphalerite was determined from cell edge measurements (Barton and Toulmin, 1966) and/or by electron microprobe. The later is more precise and shows any inhomogeneities due to disequilibrium. f_{S_2} was determined from coexisting pyrrhotite compositions by an x-ray diffraction technique (Toulmin and Barton, 1964).

Our results are in good agreement with Barton and Toulmin's extrapolations in the sphalerite-pyrrhotite binary (Table 1) indicating that FeS-ZnS is an ideal solution at least above 400°C. The usefulness of this divariant binary field as a geothermometer for natural sulfides is limited by the ability to determine f_{S_2} when deposition occurred. Pyrrhotite oxidizes rapidly in natural environments and unless it can be shown that it was well buffered, erroneous results can be obtained.

This difficulty may be overcome by examining the iron content of sphalerite in equilibrium with the well-known univariant pyrite + pyrrhotite assemblage. Barton and Toulmin showed that the FeS content of sphalerite

in equilibrium with pyrite and pyrrhotite increases with decreasing temperature from 13 mole percent at 742°C to 20 mole percent at 600°C. Analyses of natural sphalerites suggest that this curve reverses slope below 600°C, Table 2 shows that this expected reversal does not occur above 420°C and hence the sphalerite + pyrite + pyrrhotite assemblage cannot be used as a geothermometer within the temperature range investigated. Work is continuing to lower temperatures.

References

Barton, P. B., Jr. and Toulmin, P., III, (1966), "Phase relations involving sphalerite in the Fe-Zn-S system:" Econ. Geol., 61, no. 5, p. 815-849.

Toulmin, P., III, and Barton, P. B., Jr., (1964), "A thermodynamic study of pyrite and pyrrhotite:" Geochim. et Cosmochim. Acta, 28, p. 641-671.

Table IV

Sphalerite Compositions in the Sphalerite-Pyrrhotite Binary

Run	T,°C	log f_{S_2} atm.	Mole Percent FeS in Sphalerite	
			Barton & Toulmin Extrapolation	This Paper
331	578-583	- 4.5	28.4	29.4 ± 1.2
339	525-527	- 6.1	30.5	33.2 ± 1.7
327	520-528	- 5.9	25.2	25.0 ± 0.9
326	441-449	- 7.6	27.2	27.2 ± 1.8
320	393-399	-10.6	34.1	35.6 ± 1.1

Table V

Sphalerite Compositions in Equilibrium with Pyrite and Pyrrhotite

Run	T,°C	log f_{S_2} atm.	Mole Percent FeS in Sphalerite
349	522-532	-3.7	20.3 ± 0.3
353	420-431	-6.3 to -6.7	19.9 ± 0.2
354	420-436	-6.2 to -6.7	19.6 ± 0.3